Chapter 3

Charging Behavior of Clays and Clay Minerals in Aqueous Electrolyte Solutions — Experimental Methods for Measuring the Charge and Interpreting the Results

Tajana Preocanin, Ahmed Abdelmonem, Gilles Montavon and Johannes Luetzenkirchen

Additional information is available at the end of the chapter

http://dx.doi.org/10.5772/62082

Abstract

We discuss the charging behavior of clays and clay minerals in aqueous electrolyte solutions. Clay platelets exhibit different charging mechanisms on the various surfaces they expose to the solution. Thus, the basal planes have a permanent charge that is typically considered to be independent of pH, whereas the edge surfaces exhibit the amphoteric behavior and pH-dependent charge that is typical of oxide minerals. Background electrolyte concentration and composition may affect these two different mechanisms of charging in different ways. To guide and to make use of these unique properties in technical application, it is necessary to understand the effects of the various master variables (i.e. pH and background salt composition and concentration). However, how to disentangle the various contributions to the charge that is macroscopically measurable via conventional approaches (i.e. electrokinetics, potentiometric titrations, etc.) remains a challenge. The problem is depicted by discussing in detail the literature data on kaolinite obtained with crystal face specificity. Some results from similar experiments on related substrates are also discussed. As an illustration of the complexity, we have carried out extensive potentiometric mass and electrolyte titrations on artificial clay samples (Na-, Ca-, and Mg-montmorillonite). A wide variety of salts was used, and it was found that the different electrolytes had different effects on the end point of mass titrations. In the case of a purified sample (i.e. no acid-base impurities), the end point of a mass titration (the plateau of pH achieved for the highest concentrations of solid), in principle, corresponds to the point of zero net proton and hydroxide consumption, at which in ideal systems, such as oxide minerals, the net proton surface charge density is zero. To such concentrated (dense) suspensions of clay particles, aliquots of salts can be added and the resulting pH indicates the specificity of a given salt for a given clay particle system. In the experimental data, some ambiguity remains, which calls for further detailed and comprehensive studies involving the application of all the available techniques to one system. Although, right now, the overall picture appears to be clear from a generic point of view (i.e. concerning the trends), clearly, in a quantitative sense, huge differences occur for nominally

identical systems and only such a comprehensive study will allow to proof the current phenomenological picture and allow the next step to be taken to understand the fine details of the complex clay-electrolyte solution interfaces.

Keywords: Mass titration, clay mineral, montmorillonite, smectite, adsorption, acid-base properties, surface charge

1. Introduction

The charging of clays and clay minerals (hereafter referred to as clays for simplicity) is of importance in various areas. One important property related to the charging is the so-called point of zero charge. We will not repeat the various definitions of points of zero charge in detail here, but rather refer to the literature (1-3). Only the points of zero charge used in the present chapter will be explicitly defined. The books summarizing published points of zero charge of minerals include thousands of experimental studies [4, 5]. Points of zero charge can be considered sample and system intrinsic properties. In the typical compilations, the given values will indicate under which conditions (usually in terms of pH) a particle is net uncharged subject to the definition of the respective point of zero charge cited. Or, to put it otherwise, the points of zero charge indicate for which conditions a mineral surface will bear a negative or positive charge. The charge is affecting the aggregation of the particles but also the uptake of contaminants on the clays from electrolyte solutions. Most of the data that are available have been collected under ambient conditions (room temperature and ambient pressure, though sometimes carbon dioxide is excluded). This is also true for the data discussed in the following.

Well-behaved particles of oxide minerals are rather well understood with respect to their charging properties [6-8]. This is partially due to the uniform charging properties of the different crystal planes of a given particle, the domination of one specific crystal plane or that of a specific surface functional group. Clay platelets expose various crystal faces with very different properties to the surrounding solutions, which result in significant anisotropy. This is shown in a very schematic way in Figure 1.

The basal plane is often considered as a permanently charged face, which is at the origin of the overall negative charge measured for many clay platelets over the usual pH range (between pH 2 and 12). The edge faces show pH-dependent behavior as shown in Figure 1, and this results in the anisotropy of the particles with respect to charging behavior and charge. Therefore, compared to the oxide minerals, a number of complications exist, which will be discussed in more detail in the following.

For the basal planes, the following can be generally stated:

- Basal planes exhibit permanent, negative charge that, in the common picture, arises from the isomorphic substitution within the particles and is typically not expected to depend on the proton concentration. At extreme pH values, some dependence on pH will occur if one believes in current models [9], but experimental data that will be discussed later also suggest effects in the usually studied pH range.

http://dx.doi.org/10.5772/62082

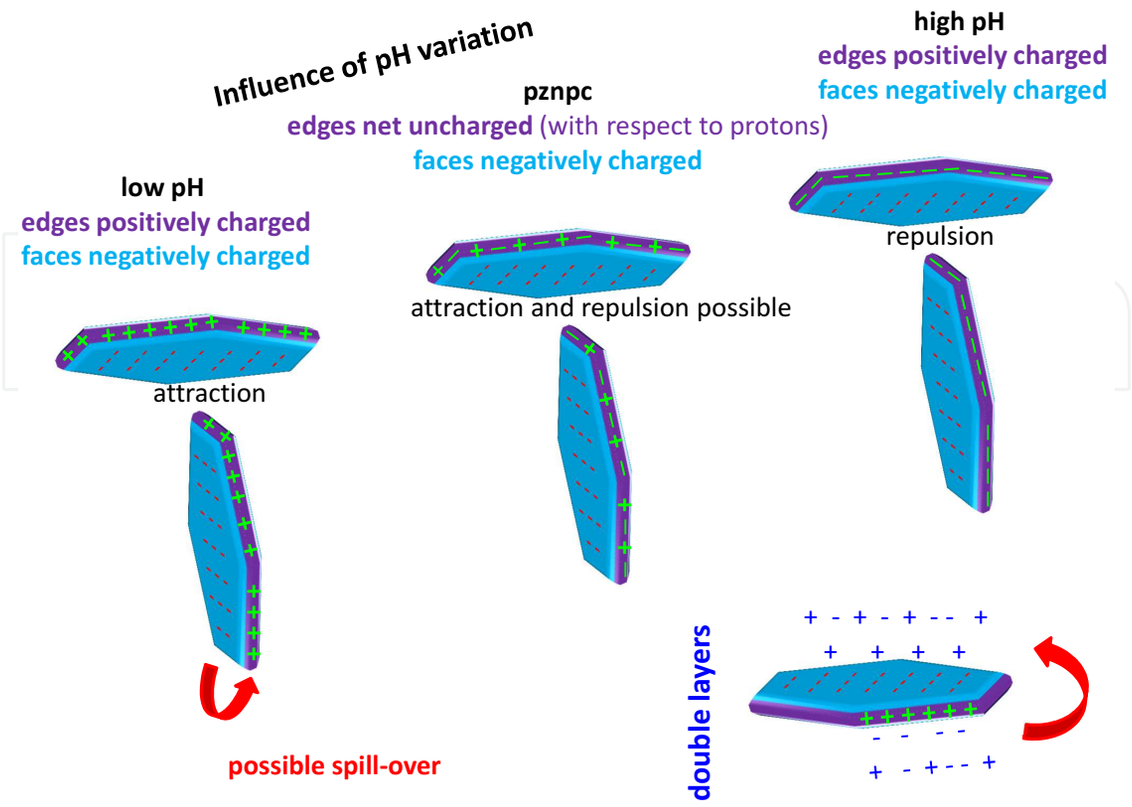

Figure 1. Schematic view of clay platelets and their anisotropic charging behavior. The faces (basal planes) exhibit permanent negative charge, whereas edge faces show amphoteric, pH-dependent behavior similar to oxide minerals. The anisotropy causes, depending on the pH and the concomitant charge of the edge faces, possible attraction (at low and intermediate pH values) or net repulsion (at high pH values). The respective charging conditions may cause aggregation (in some kind of card-house structure) and will involve spillover situations, which, in turn, affect the electrical double layers.

- There might be different basal planes (such as on kaolinite, with a gibbsite plane and a silica plane) with different charging properties.
- The permanently charged basal surfaces are affected by salt concentration.

For the edge surfaces, the generally accepted viewpoint is similar to that for oxide minerals and can be summarized as follows:

- The amphoteric clay edge surfaces expose hydroxyl groups to the solution, which may take up or release protons depending on the nature of these groups and on the proton concentration in solution. There is a specific pH at which the net charge on such surfaces is zero, which can be called the "point of zero net proton charge" [2] (pH_{pzcnpc}) and has also been termed "point of zero net proton consumption" [10].[1]

1 As indicated above, there is a somewhat confusing nomenclature within the literature, which requires to assign a clear definition to whatever point of zero charge is discussed; here, the definition would be that, on the specific surface that is being discussed, the net charge arising from proton adsorption and desorption in the plane of the surface hydroxyls is zero. Furthermore, it is inherently assumed that the adsorption/desorption of protons and hydroxide ions in other parts of the interface can be neglected.

- Again, the situation may be complicated by the occurrences of various clay edge surfaces with different properties on a given particles (i.e. different values of pH_{pznpc} may appear on the edges of one clay particle).

Another yet distinct mechanism occurring on these particles is (cat)ion exchange.

- Whereas some clays (such as kaolinite) do not exhibit strong interlayer cation exchange, others (such as montmorillonite or illite) possess relatively high cation exchange capacities.
- Exposing the latter to strongly concentrated electrolyte solutions will cause an exchange of the interlayer ions (i.e. exposure of a sodium clay to a sufficiently concentrated calcium solution will transform the clay to the calcium form at equilibrium) and was shown to have repercussions on modeling metal ion adsorption [11].[2]
- At very low pH, the solid can be transformed to its H-form, which will involve a substantial buffering capacity.

The impact of the master variables pH and ionic strength on these particles becomes highly complex. The formation of the so-called electrical interfacial layer (EIL) of charged particles in aqueous solutions is one central aspect [12]. The more distinct properties a certain clay possesses, the more complex the overall behavior will be. We briefly discuss the effect of electrolyte concentration and composition before discussing the role of pH.

- The formation of the EIL on a single crystal plane is defined by the overall surface charge density (immobile, Stern layer) and the diffuse layer properties (electrolyte composition and concentration). The former arises from the specific adsorption of potential/charge-determining ions and/or the permanent charge due to isomorphic substitution. Electrolyte ions may have twofold effects. First, they may form ion pairs with the charged surface and thus screen the charge within the immobile layer. The higher the affinity of a given ion to a specific surface is, the more effective the screening will be. Sufficiently high affinity may lead to overcharging (i.e. charge inversion). Second, electrolyte ions will neutralize the net charge of the immobile layer in the diffuse part of the EIL. The higher the charge of an ion is, the more effective the screening will be. Increasing the electrolyte concentration will enhance screening.
- The ion-exchange properties are obviously also dependent on the salt concentration. Thus, studying the behavior of a Na-clay in high concentrations of calcium or some other cation different from sodium will transform the clay either partially or completely into another form, similar to what happens at low pH as discussed above.
- Protons are potential/charge-determining ions on the clay edge surfaces, where they adsorb or desorb from surface hydroxyl groups. They may also play a role in ion-exchange reactions if the pH is sufficiently low (i.e. the proton concentration is sufficiently high). Basal planes are, in many cases, not prone to reactions with protons in a wide range of pH. Model

2 In this example with high relevance, the form of the given clay resulted in different properties with respect to contaminant adsorption, an issue that is presently not solved within an otherwise consistent model. As an unsatisfactory way out, the stability constants for Eu adsorption are different on Na- and Ca-montmorillonite for identical reactions, which causes problems for mixed Na/Ca systems.

http://dx.doi.org/10.5772/62082

calculations suggest such behavior from pH 3 to 10 for the gibbsite basal plane, which occurs as aluminol terminated face on kaolinite and therefore is quite relevant [13]. Unfortunately, experimental data for and consequently the interpretation of this seemingly simple surface are still quite diverging for unknown reasons [13-17]. However, there are some observations in the literature that would suggest additional effects of protons (or hydroxide ions) on such basal planes [18].

Various macroscopic measurements on the effects of electrolytes and protons on clay surface charging exist. The major techniques are titrations, electrokinetic experiments, measurements of the cation exchange capacities, or adsorption studies. These measurements test different chemical reactions. Among the titrations, various techniques can be used. For a detailed recent overview, we refer to the literature [19]. Electrokinetic techniques have also been reviewed frequently [20]. We will not discuss the two other techniques mentioned above, because they are only indirectly related to the charging.

- Classical potentiometric acid-base titrations both in terms of evaluation of the raw data and thermodynamic modeling involve proton balances. For an accurate treatment of the raw data, all the reactions occurring in a given system need to be known and their respective extents need to be quantified. Quite importantly for the interpretation of the measurements, secondary effects on pH may occur that also will affect the overall proton balance. This includes the dissolution of the particles and subsequent reactions of the freshly dissolved species in solution. As is the case when changing the electrolyte concentration, a multitude of reactions involving solutes may occur when changing the pH. Re-precipitation may occur (of primary or secondary phases). Dissolved species may adsorb, as has been discussed for aluminum ions on gibbsite-basal-plane-like surfaces [17]. Also, it becomes difficult, if not impossible, to disentangle the concomitant origins of a macroscopic scale observation, as all these processes have their own, sometimes unknown, pH dependencies.

- Mass and electrolyte titrations [21-23] are far less frequently applied, and we will therefore devote a part of this chapter to these kinds of experiments. They involve relatively high mass concentrations, which will supress the relative importance of the secondary reactions (such as dissolution, precipitation, or (re)adsorption of previously dissolving clay components) in the overall proton balance. As a an example, the dissolution of a given particle into a thick suspension will not cause the same effects as in a dilute suspension. In the latter, much more has to be dissolved (in absolute terms) to achieve a solubility equilibrium compared to the thick suspension.

- Electrokinetic measurements (such as electrokinetic mobility) test the movement of a particle in an applied electric field. The resulting mobility is caused by the behavior of the overall particle. This may be very complex. The available set-ups will produce a value for the electrophoretic mobility. The value typically used, however, is the so-called zeta-potential. The transition from the former to the latter is not simple for non-spherical particles. It may be even more complex for anisotropic particles such as clays.

The anisotropy has been alluded to above and is caused by the crystal face-specific properties of the overall particles. Only recently, more face-specific work has become available (see

Chapter 2) on anisotropic particles. Crystal face-specific effects have been acknowledged for a long time. Early examples of general importance [24] or specific work on oxides [25] can be consulted. The differences in charging on the different crystal planes may have significant consequences on the overall charging.

- Depending on the size of the surfaces with different properties that contribute to the overall exposed surface area, macroscopic observations can be described using various assumptions [26]. The approaches discussed in that reference and also in the literature cited therein consider a common diffuse part of the double layer.
- It is well conceivable that, with sufficiently large patches, distinct diffuse layers may evolve, resulting in repercussions on inner-layer equilibria and local effects. The consequences of these effects are not well established, although spillover effects have been discussed with respect to clays [27, 28]. Only more recently, an approach based on MD simulations and thermodynamic modeling has addressed montmorillonite [29, 30]. Interesting and challenging questions can be asked about the relevance of these double layers at the locations, where the transition from plate to edge occurs in such cases (i.e. whether and how the changes will affect the equilibria of adsorption and dissolution).
- Another issue would be how different surface potentials on one particles are related via the bulk of the solid [31] and how this may affect reactivity [32]. Probably, this is not a major issue for clays and more relevant to solids with sufficient electrical conductivity.
- Moreover, the effects of interfacial water molecules and water ions (H^+ and OH^-), especially on the basal plane, should be taken into account [33]. It is known that the physical and chemical properties of water change close to such interfaces, and for example, the ionization of water molecules becomes more pronounced [34].

The association of the various measurements with a specific property in the EIL is one of the challenges (i.e. what quantity is actually measured, what property is tested, and which interdependencies exist between the properties and quantities). Things are further complicated by the fact that the overall properties are finally relevant to processes such as aggregation (i.e. does aggregation of particles occur), the morphology of the aggregates formed (i.e. how do the particles interact with each other), the interaction of the particles with other surfaces (i.e. by which particle face is a clay particle attached to any kind of surface), or the interaction of solutes with a particle (i.e. on which particle face is a contaminant ion bound), to only name a few. Just to give an illustration of the potential difficulties, we can cite a study that has shown that heterogeneously charged particles may move in an applied electric field, although their net surface charge (relevant for electrokinetics) is zero [35]. Because such work is predominantly of theoretical nature, recent activities have turned towards experimental approaches. Surface plane-specific investigations are possible by the study of single crystals [exposing only one specific crystal plane, usually sufficiently large samples need to be available as was the case for gibbsite [14] or is the case for many single crystal samples of oxides including sapphire, hematite [36, 37], mica [38, 39], and others] or by exposing distinct crystal planes from small particles in an intelligent way to force probes [as recently published for gibbsite [40] and

http://dx.doi.org/10.5772/62082

extensively done with kaolinite [41-44]]; the major problem remains the edge part of the clays due to their small dimensions).

Overall, it appears that experimental techniques for studying the interfacial properties of clay particles have made a significant leap forward beyond the macroscopic approaches. The more sophisticated approaches that are plane specific require detailed technical knowledge and instrumentation, whereas the macroscopic approaches are more standard although not necessarily simple. Unfortunately, at present, a combined study involving the available experimental and theoretical approaches on the different scales on a defined sample has not been performed in a comprehensive way.

Here, we will describe in detail the case of kaolinite where the use of crystal face specificity has been driven quite far [42-44] and add some information on other minerals where the approaches have been applied as well before describing non-conventional but very simple titration methods in more detail. In the part dealing with macroscopic methods, a synthetic clay has been used to assure a well-controlled starting material, free of impurities that are associated with natural samples and that, in turn, require specific preparation protocols.

Although the advances in the experimental techniques allow the specific study of defined crystal planes with more (basal plane surfaces) or less (edge surfaces) confidence, the problem remains, for example, how to assemble the detailed information for the defined crystal planes in reconstructing the overall behavior such as the titration curve or the zeta-potentials. Early attempts on obtaining zeta-potentials for kaolinite in such a way exist [45, 46]. On the other extreme, the advent of modern theoretical approaches has allowed to calculate protonation constants for surface functional groups on ideal surfaces, some studies notably including phyllosilicates [47]. Such information is quite compatible with results from advanced surface complexation models [6] and can, in principle, be used to construct a model to predict the overall clay behavior involving the problems of how to couple the different planes. Using the crystal face-specific information obtained, protonation constants can be more directly tested in a first step. This is the goal of the following sections, where we also point to experimental problems. First, we will discuss in some detail the available experimental face-specific data on kaolinite and relate them to the theoretical results, complemented by similar data on talc. Second, we will discuss the basal plane of mica in some detail. The final chapter describes some experimental data from mass and electrolyte titrations showing the complexity that will have to be considered in constructing comprehensive models for clay particles that take into account the microscopic reactions and their associated stability constants and the various phenomena involved plus the "interactions" between the different facets.

2. Kaolinite as an example

2.1. Effect of pH

As indicated in the introduction, the most well-studied system from the point of view of interfacial charge is probably the kaolinite sample investigated by Miller and co-workers

[41-44, 48]. Here, we briefly review the outcome of that comprehensive study. The challenging steps in this study included the preparation of kaolinite particles, such that they would expose the silica or gibbsite basal faces to the atomic force microscopy (AFM) probe and design an experiment by which to measure the behavior of the edges. The dimension of the edge planes (below 50 nm) is a major obstacle. Compared to the edge surfaces, the basal surfaces have much larger extensions. Also, the basal planes can probably be considered smoother than the edge surfaces.

2.1.1. Basal plane surfaces

In the above-cited studies, the basal surfaces were attached to a larger single crystal surface (serving as a supporting material). One single crystal was a fused alumina surface that was expected to have a high isoelectric point and to exhibit positive charge over a wide pH range. Moreover, it was anticipated that the silica plane of kaolinite would exhibit a negative charge. Thus, having a kaolinite particle interact with a positively charged single crystal, it would attach via the silica basal plane to the single crystal. Consequently, it would expose its gibbsite plane to the AFM probe, allowing to measure the distinct properties of the kaolinite-gibbsite plane. Applying the same approach but using a glass substrate as a support with a low IEP[3] (below pH 3), which makes it negative over a wide pH range, would allow to fix the gibbsite plane of the kaolinite particles to the supporting surface and thus expose the silica plane to the solution. The AFM probe was a conventional silicon nitride tip with widely known properties. Measurements were made in a fluid cell.

The outcome of the measurements with the distinct planes was that the gibbsite plane had an IEP from force measurements that corresponded to pH 6, whereas that of the silica plane was below pH 4.

These measurements can be compared to independent measurements or predictions. Gibbsite has been separately investigated in various studies. In particular, a similar AFM study on the basal plane of gibbsite particles was carried out. The various surfaces on kaolinite and their relations to gibbsite and silica as well as the situations for the force measurements (which typically involve a silica probe) are shown in Figure 2a. The results of the separate force studies are shown on Figure 2b.

Clearly, all data sets show positive potentials at pH <6. This disagrees with predictions for the protonation constants of the doubly coordinated hydroxyl groups that occur on this surface both by MUSIC [16] and by advanced theoretical calculations [51]. However, it should be noted that the potentials are quite low, in particular for the gibbsite study, which would imply low surface charge. Likewise interesting is that (i) the positive potential differs significantly from each other (those obtained on kaolinite are much larger in one case) and (ii) there is a charge reversal on kaolinite, whereas, on the gibbsite basal plane, there is none in the pH range investigated. The kaolinite data differ among themselves as well, although the same material

3 The IEP in our notation corresponds to the pH at which the zeta-potential or the DLVO potential is zero. DLVO potentials are interfacial potentials at the head end of the diffuse layer.

http://dx.doi.org/10.5772/62082

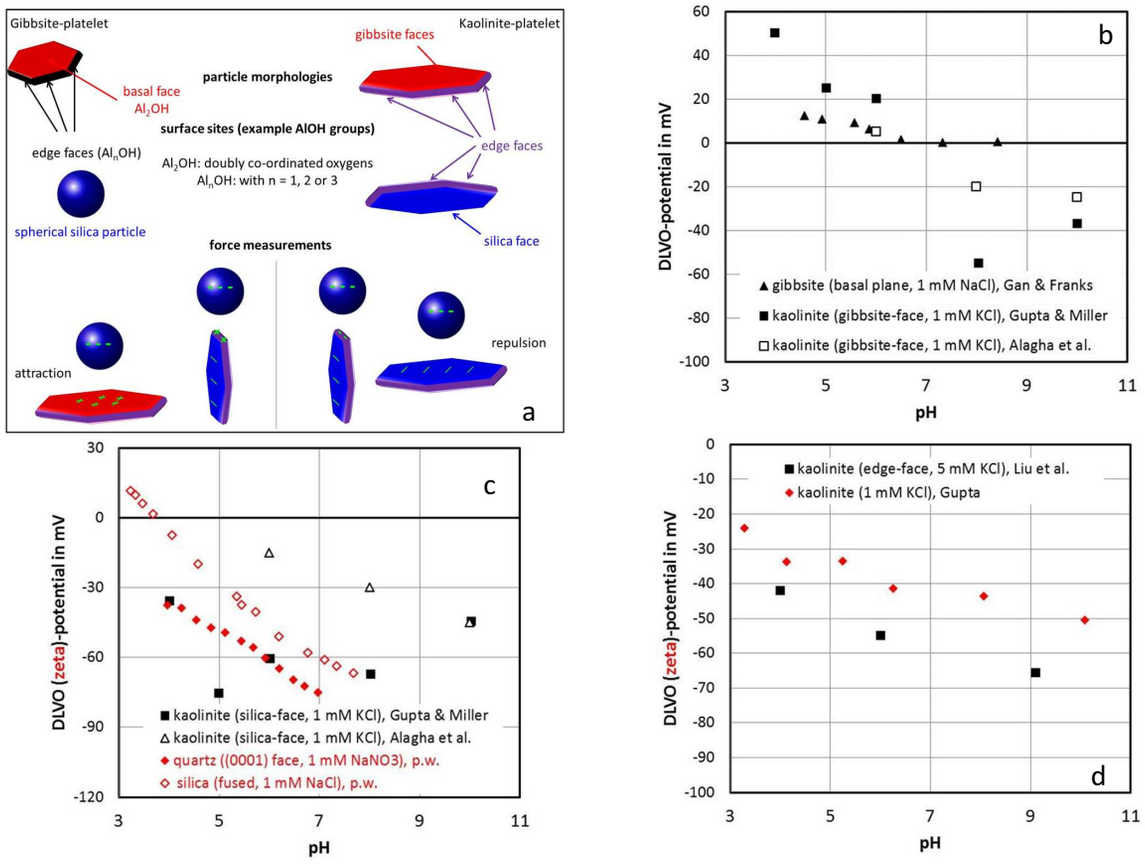

Figure 2. (a) Faces on kaolinite and their relations to oxide minerals and typical situations for force curves. (b) DLVO potential measured by AFM force distance curves on the gibbsite plane of kaolinite [42, 49] and on the basal plane of gibbsite [14]. (c) DLVO potentials (full black squares and open triangles) measured by AFM force distance curves on the silica plane of kaolinite [42, 49] and zeta-potentials (diamonds, red symbols) on the (0001) plane of quartz and fused silica (present work). (d) DLVO potential (black squares) of kaolinite edge surfaces in 5 mM KCl [44] and zeta-potentials (red diamonds) of the same kaolinite particles in 1 mM KCl [50].

was used. Note that electrolyte concentrations are equal in both cases, in KCl (kaolinite) and NaCl (gibbsite).

The disagreement on both experimental data and interpretation of the gibbsite basal plane has been ongoing for some time. The origin of the discrepancies in the experimental data has been discussed in some detail, but the issue is still not solved [13, 52, 53]. Adsorption on the gibbsite plane of either dissolved aluminum [17, 52, 54, 55] or background electrolyte [40] ions has been put forward or inferred from experimental data. Interpretation obviously is linked to the experimental data basis, and likewise, no agreement has been achieved.

The silica basal plane of kaolinite shows the expected results if one assumes that silica is usually negatively charge above pH 2. This is exemplified on Figure 2c by data series for the 0001 plane of quartz obtained by streaming potential measurements in 1 mM $NaNO_3$. Streaming potential measurements with a fused silica sample in 1 mM NaCl yield absolute zeta-potential values that are slightly lower than those of the quartz sample. Clearly, the data are in agreement in that they remain negative for nearly all measurements carried out. At the lower pH range, they

match very well. Independent data by Alagha et al. [49] on the same system are different and only coincide at pH 10.

2.1.2. Edge plane studies

For the determination of the IEP of the edge surfaces, samples of well-ordered kaolinite edge surfaces were prepared as an epoxy resin sandwich structure having layered kaolinite particles in the center of the epoxy resin sandwich [44]. The resulting samples always showed negative diffuse layer potentials (less than -40 mV in 5 mM NaCl solutions as shown in Figure 2d), which is rather surprising given that the points of zero net proton charge[4] based on potentiometric titrations as recently summarized by Liu et al. [56] were assumed to be between pH 5 and 6. Additional zeta-potential data from Gupta [50] do support an overall low IEP for the very same particles.

The important point to realize here is that potentiometric titrations at best yield relative surface charges, but these also include potential contributions from both basal planes, and a precise procedure of calculating the overall charge is not known. To put the data on an absolute scale, various approaches can be taken. On oxide minerals, a common intersection point of such relative charging curves occurs and typically coincides with an independent determination of the IEP and then the pristine point of zero charge emerges. Furthermore, referring again to Figure 3, the zeta-potentials in lower salt content measured for the metal oxide particles exhibit lower absolute values than the DLVO potentials of the edges in the more concentrated salt solution. Even if one might still argue that the DLVO potentials can be higher than the zeta-potentials [57], the observation could suggest that the pH dependence and absolute values for the kaolinite particles here originate from the edges only.

Including Figures 2b and 2c, this would mean that the basal planes should neutralize each other from a simple point of view, although they could still cause a finite zeta-potential [58]. This, in turn, would contradict the point of zero salt effect[5] of kaolinite determined by Gupta [50] in KCl, which is at pH 4.5. The assignment of a clear point of zero net proton charge based on the data shown in Figure 3 is not as simple with clays, as it usually is the case with oxides. First, the apparent zero level shifts with both the electrolyte concentration and the amount of kaolinite titrated. Second, a common intersection may occur at pH 7. If only the edge surfaces were responsible for the pH-dependent charging, the point of zero net proton charge would be clearly below pH 4, whereas the salt titration and the relative zero level would suggest it to be at pH 4.5.

For clays as discussed in detail above, there are several contributions to the overall charge and a common intersection point does not give the point of zero net proton charge. The charging curves are affected by the net charge that influences given surface functional groups. The distinct behavior of the different planes in terms of diffuse layer potentials is shown in

4 For the five samples with generic sites, we calculate a mean of 5.7 with a standard deviation of 0.7 (the maximum being 6.8 and minimum being 5.0).

5 The point of zero salt effect is the pH at which the addition of salt does not cause a change in surface charge density. This is likely to happen at zero surface charge for well-behaved particles.

http://dx.doi.org/10.5772/62082

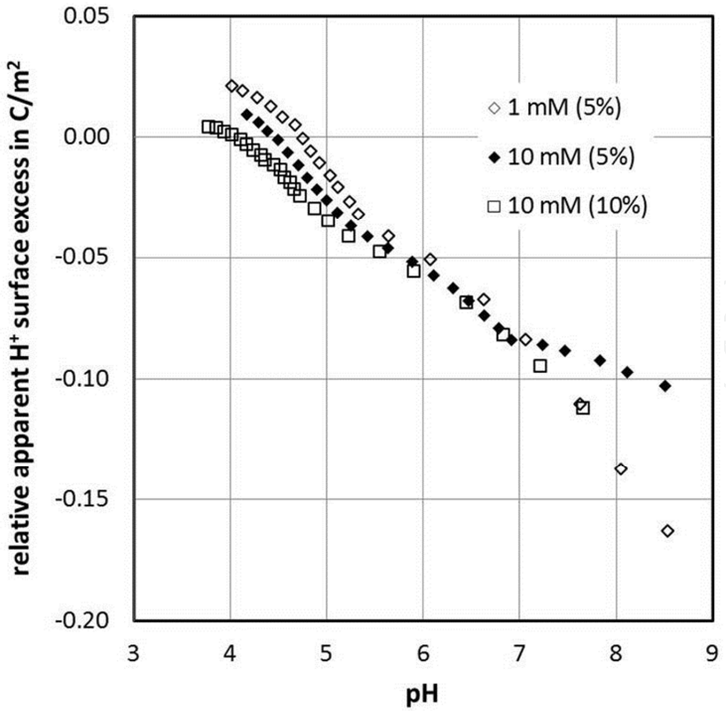

Figure 3. Titration of the kaolinite sample used for the AFM force distance measurements shown in Figures 1 and 2 [50]. The percentage refers to the weight of kaolinite in the titrated suspension. Salt was KCl.

Figure 4. Surprisingly, the silica basal plane and the edge plane are very similar, in particular with respect to the zero-potential condition. This could mean that the silica groups at the edge surface are dominating. The traditional view is that both alumina and silica groups are present and that the point of zero net proton charge of edges should be higher than reported here.

In summary, it is clear that both the gibbsite and the silica basal plane exhibit pH-dependent behavior, suggesting proton uptake and/or release from the surface functional groups on the two planes. This is surprising because the expected surface functional groups are usually expected to be inert towards the reactions of protons within the normal pH range. The lack of agreement on this issue for the gibbsite basal plane has been mentioned above. Based on the available data, the overall charging behavior is difficult to estimate because investigations on the basal planes were done in 1 mM NaCl media. The obtained diffuse layer potentials would be larger in value than in 5 mM NaCl, which was the medium in the experiments dealing with the edge faces. An overall estimate would be possible using the estimated diffuse layer charge densities and the respective areas to calculate an overall diffuse layer charge density on the particle. From this, one may estimate a new diffuse layer potential for comparison with the independent measure of zeta-potential for the particles, where the measurement device yields data that are in an unknown fashion obtained from the anisotropic particles. We also would like to mention here that similar studies are available in terms of pH dependencies on other clay materials [59, 60]. Without going into further details of this pH-dependent study, we turn the attention to the effect of electrolyte concentration at constant pH.

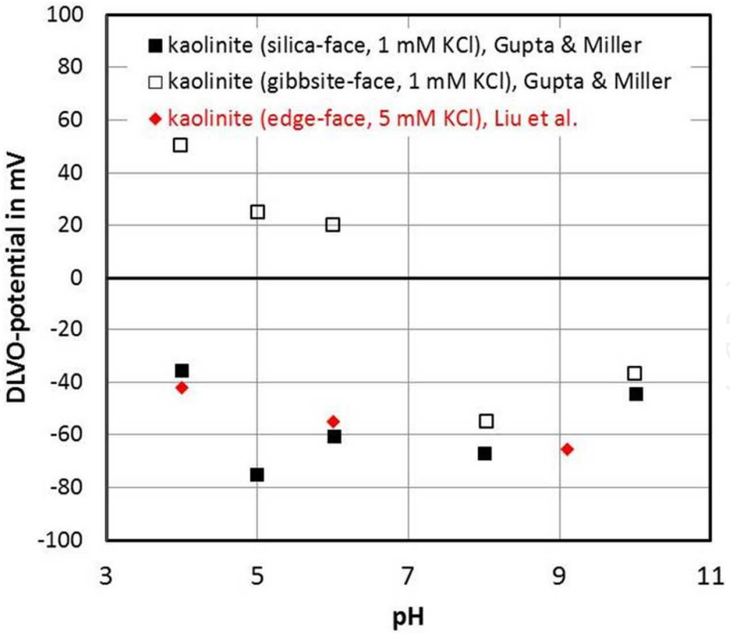

Figure 4. Comparison of the potentials on the different faces of kaolinite as a function of pH [42, 44].

2.2. Effect of ionic strength

A similar series of experiments as the one described above for the effect of pH has been carried out at a given pH for a variation of the electrolyte concentration. As a first step, a proof of principle has shown the consistency between diffuse layer and zeta-potentials among probe and a supporting surface [44]. The zeta-potentials were found to be smaller in magnitude than the diffuse layer potentials, suggesting that the zeta-potentials pertain to a location slightly shifted towards the solution side of the particle in agreement with independent work [16, 57]. The AFM force distance curve-based diffuse layer potential is at the head end of the diffuse layer and is attenuated towards the solution due to screening by the background electrolyte. For silica particles, the data follow the same trend but are just shifted, the shift decreasing with increasing ionic strength. For the kaolinite study at pH 5.6 [44], the results are shown in Figure 5a.

The data can be summarized as follows. The diffuse layer potential on the gibbsite plane is positive, remains roughly constant, and only decreases at the highest salt concentration. On the silica plane, the negative potential becomes less negative with increasing salt content and then remains approximately constant. The value for the edges is roughly constant and negative. The potentials on the gibbsite and the silica and edge planes are 20 and -30 mV, respectively, with little salt dependence in the range of ionic strength that was studied (except for the silica plane at very low salt content). As pointed out before, the overall zeta-potential estimation requires a recalculation of the diffuse layer charge densities from the measured potentials and area-weighted summation of the contribution. With the assumption that the gibbsite and silica planes have roughly the same area and within the experimental errors given, the charge from those two planes cancel each other at approximately 10 mM. Then, the edges would be solely contributing to the overall charge, resulting in a charge density (referred to as

http://dx.doi.org/10.5772/62082

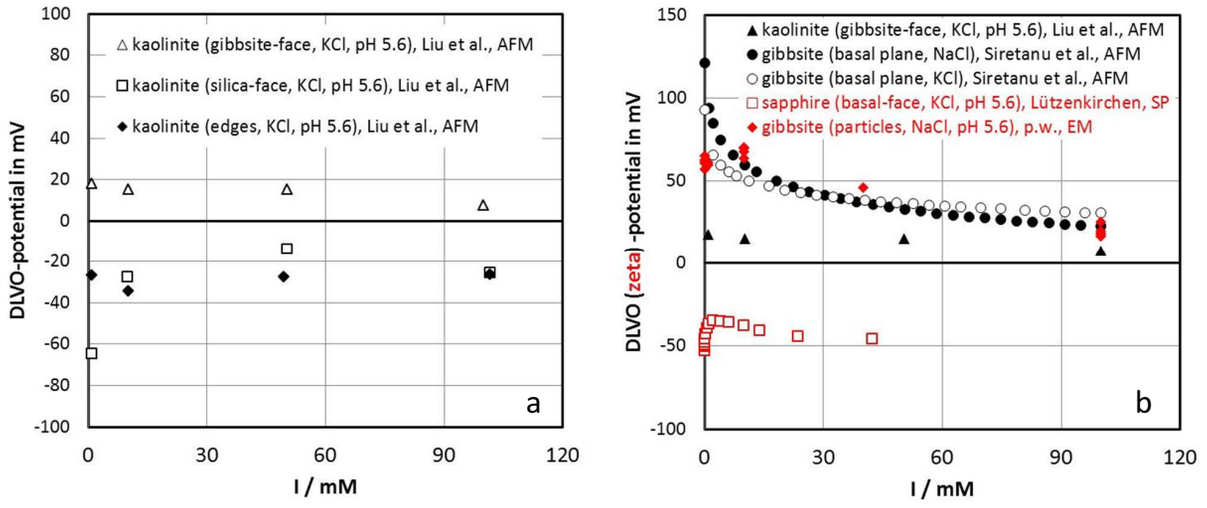

In the following, we will use in the figure legends the abbreviations AFM (atomic force microscopy), SP (streaming potential), EM (electrophoretic mobility), SFA (surface force apparatus), PIT (plane interface technique), and p.w. (previously unpublished data from the present authors).

Figure 5. (a) Salt dependence of DLVO potentials of the different kaolinite faces. Data from Liu et al. [61] were all determined by AFM force distance measurements. (b) Interfacial potential for gibbsite basal plane-related surfaces at pH 5.6 as a function of salt concentration (given as ionic strength). Data are for the gibbsite face of kaolinite from Liu et al. [61], for the gibbsite basal plane from Siretanu et al. [40], and for the sapphire basal face from Lützenkirchen [62].

the edge area) of approximately -10 mC/m^2. Scaled to as the overall surface, this would be much lower resulting in an overall diffuse layer potential below -20 mV in 10 mM salt. The zeta-potential measurement under these conditions is not available for the very same sample. For 1 mM background electrolyte concentration, a value between -30 and -40 mV can be inferred from the thesis of Gupta [50]. Therefore, the range appears reasonable, although a self-consistent comparison again is not possible for lack of data. At 50 mV, the situation for the gibbsite and silica basal planes is similar [44] and the resulting reported charge density (scaled to as the edge area) yields a value of -15 mC/m^2. Nothing can be further inferred from this result though. Finally, it has also to be acknowledged that the recalculation of diffuse layer potentials from overall charges involves geometry. The same is true for the calculation of zeta-potentials from electrophoretic mobility. Consequently, much can be done to improve the present attempts to gain insight in the effect of crystal plane-specific charging on overall charge. Interestingly, the silica and the edge planes are very similar again.

The salt dependencies of the two basal planes are compared to related surfaces in Figure 5b (gibbsite face) and Figure 7 (silica face). We first discuss the gibbsite face and some additional data on pure gibbsite particles.

Figure 5b shows that there is quite close agreement between gibbsite samples for pH approximately 5.6. True gibbsite particles that are dominated by the basal plane exhibit high zeta-potentials and a characteristic maximum at millimolar concentration. This is reminiscent of published AFM charge data on the basal plane of gibbsite [40][6] and is also retrieved on sapphire single crystals [62], though displaced to negative values. It has been pointed out previously that the gibbsite basal plane appears to be rather complex when exposed to aqueous solutions.

As a further example of the complexity, we present data that show the evolution of the conductance of the gibbsite particles corresponding to the data in Figure 6a in MilliQ water with time (Figure 6b) as well as the concomitant sample zeta-potential (Figure 6c). The conductance increases with time. This could be caused by two effects. One would be a leakage of KCl from the glass electrode. Alternatively, Al could dissolve from the gibbsite and (partially) re-adsorb as has been speculated previously [17, 52, 54]. Figure 6c shows that the zeta-potential remains high and does not show the decrease that is found when adding NaCl (Figure 5).

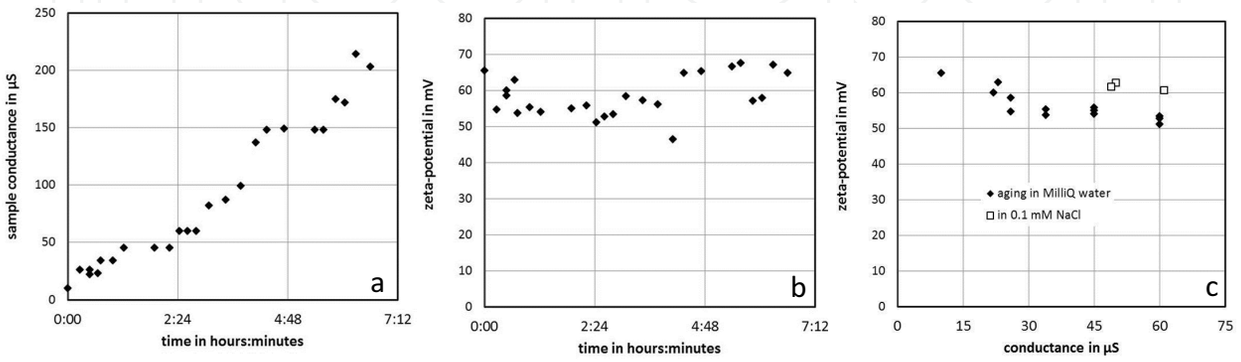

Figure 6. (a) Conductance of a gibbsite suspension in MilliQ water at pH 5.6 as a function of time. (b) Zeta-potential of a gibbsite suspension in MilliQ water at pH 5.6. (c) Zeta-potential of a gibbsite sample in MilliQ water when aged as a function of the conductance in comparison to a sample in 0.1 mM NaCl yielding a conductance in the relevant range.

Figure 6c shows a comparison between data at the lower end of conductance and compares the trend to a suspension freshly prepared in 0.1 mM NaCl, which gives rise to a similar conductance. Clearly, the zeta-potential is higher in the case of NaCl addition, supporting the idea that the increase in conductivity arises from dissolution of gibbsite. The overall trend in zeta-potential of the particles shown in Figure 5b appears to be more difficult to understand and would be the consequence of the various processes that occur. In themselves, these processes involving dissolution, re-adsorption, or even re-precipitation are complex, and these processes and the effect of added salt could also cause changes in pH.

The situation with respect to the silanol face is shown in Figure 7. Interfacial potentials are negative, but the range can vary widely. The data in Figure 7 are by no means exhaustive. There is a wealth of data available both from force curves[7] or zeta-potentials.

2.3. Summary of the kaolinite study

Despite the huge step forward to characterizing individual surface planes of distinct particles in terms of charging, there is ample space for improving the experimental data basis. Also, the kaolinite study has opened a plethora of new questions, one being why the observed kaolinite

6 We note that it is not possible to directly compare the trends in the charges and potentials. In the cited work, the potentials were not reported. We obtained the DLVO potentials from Igor Siretanu (University of Enschede).

7 Silica is a popular tip material in AFM force distance studies either directly or as a consequence of Si3N4 oxidation.

http://dx.doi.org/10.5772/62082

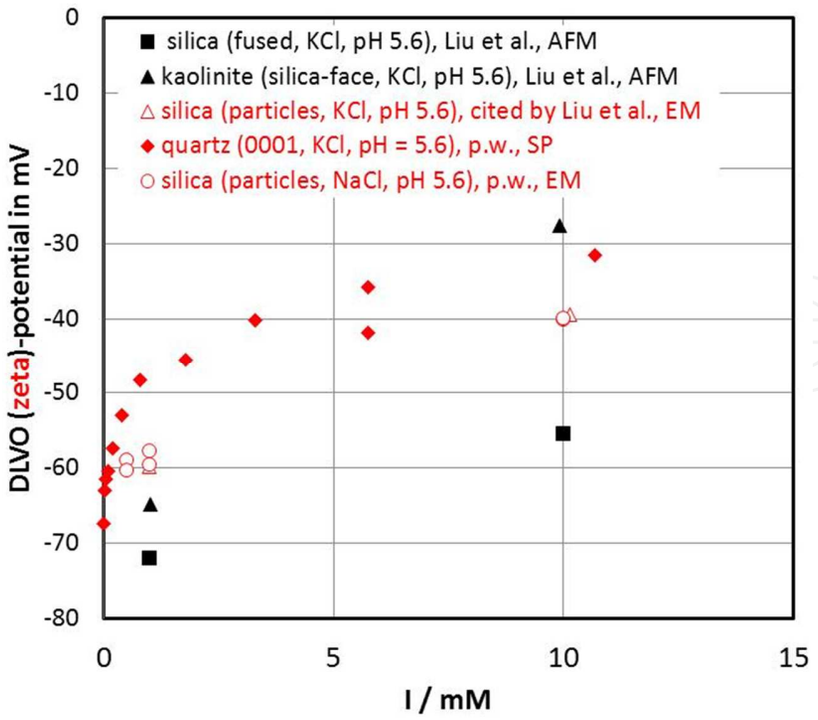

Figure 7. Interfacial potentials of silica relevant to the kaolinite silica plane as a function of salt concentration (equivalent to ionic strength in the case of the monovalent salts) at pH 5.6. Kaolinite and fused silica data are from Liu et al. [61]. Data for silica (AFM tip) are from Siretanu et al. [40]. Data for silica particles are those cited by Liu et al. [61] from previous literature.

edge surface chemistry with an IEP below pH 4 disagrees with all previous estimates of the point of zero net proton charge of above pH 5. It also disagrees with the theoretical estimates which suggest a pK of 5.7 [56]. Noteworthy, the determination of the edge face IEP was done by excluding the basal planes. The same could be said about the determination of the properties of the basal planes themselves, in which case, however, the edge planes were not excluded. Ideally measurements were made sufficiently far from the edges. The study of different sizes of the otherwise identical particles could shed light on possible surface potential effects.

3. Further direct evidence for the anisotropy of other clay minerals

3.1. Mica

3.1.1. Mica basal plane

The mica basal plane is probably one of the most frequently studied single crystal surfaces. Because it can be prepared as an atomically flat sample, it is suitable for a range of sophisticated methods that are not applicable to rougher surfaces, including X-ray reflectivity [38, 39, 63], high-resolution AFM that is able to show hydration layers [64], or ions on mica [65] or nano-ultrasonics [66], to name a few such approaches. The literature on macroscopic data on mica

is also abundant. The present work is therefore not citing all the available work and comparing all available data.

Figure 12 shows data for mica at constant pH for variable salt levels of KCl. The data for the higher pH deviate, whereas the remainder of the data is in a common cloud independent of the method. Similar data are shown for a constant salt level and pH variation in Figure 9a. There is clear agreement about the level of the interfacial potential at pH >5.5, except for the data obtained using the plane interface technique (PIT). An important difference occurs at the lower pH range, where the IEP would be obtained. Depending on the source, the slope of the interfacial potential with decreasing pH differs a lot, resulting in different IEPs for the samples under investigation. Additional data on ionic strength dependence are shown in Figure 9b involving different salts.

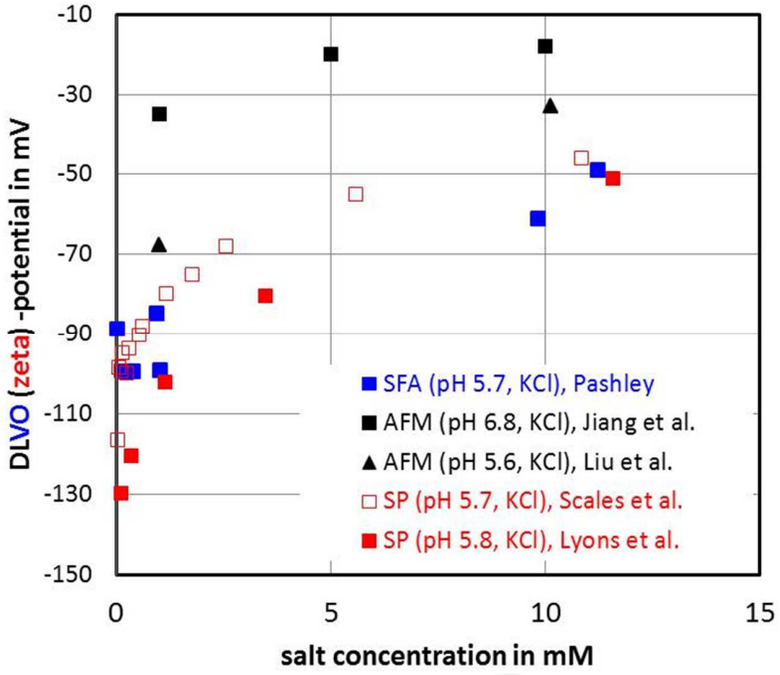

Figure 8. Zeta-potentials (red) and DLVO potentials of mica as a function of salt concentration at near-neutral pH in KCl solutions. SFA data are from Pashley [67]. AFM data are from Jiang et al. [59] and Liu et al. [61]. Streaming potential data are from Scales et al. [68] and Lyons et al. [69].

The possible origins of the differences include aging according to Lyons et al. [69] as shown in Figure 10a for mica particles and for freshly cleaved mica basal planes that were subsequently aged. Clearly, aging in both cases strongly increases the IEP. Figure 10b also shows that freshly cleaved basal planes do not necessarily yield unique IEPs. There is significant scatter, and there is some discussion in the literature about how to prepare these surfaces. Figure 10c shows similar results for uncleaved mica basal planes. Again, there is clear scatter for mica samples from the same source. Also, the IEP is higher than for the freshly cleaved surfaces. This is consistent with the results obtained on aging of freshly cleaved samples. Overall, aging (whether on freshly cleaved samples or simply due to the use of aged samples) results in the deviation from the consistency that was noted in Figures 8 and 9a for pH >5.5. Besides these

http://dx.doi.org/10.5772/62082

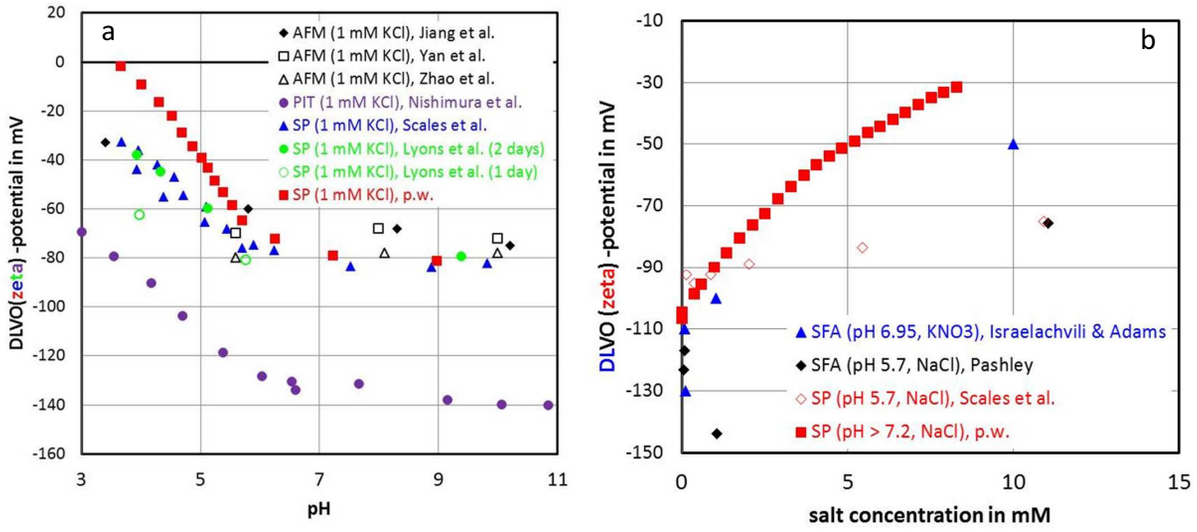

Figure 9. Zeta-potentials (colored) and DLVO potentials of mica as a function of pH in 1 mM KCl solutions (a) and in other monovalent salts (b). Data in Figure 9a are from Jiang et al. [59], Yan et al. [70], Zhao et al. [60], Nishimura et al. [71], Scales et al. [68], and Lyons et al. [69]. Data in Figure 9b are from Pashley [67], Israelachvili and Adams [72], and Scales et al. [68].

preparation-related differences, the origin of the mica itself has also been shown to affect the results as discussed in some detail by Lyons et al. [69]. Therefore, mica data should best be compared if the source of the sample and the preparation of the surface under investigation were identical.

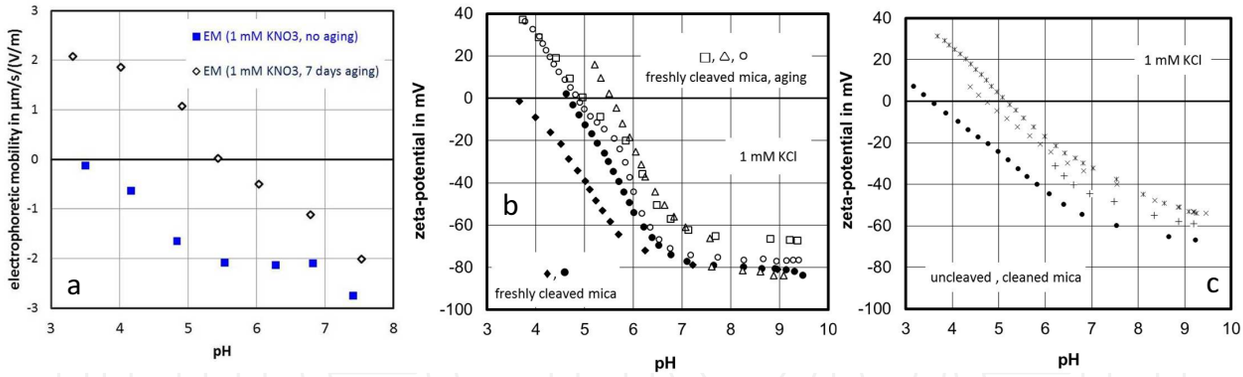

Figure 10. (a) Electrophoretic mobilities of mica particles at different aging times from Lyons et al. [69]. (b) Streaming potential data for mica basal planes in 1 mM KCl, freshly cleaved and aged. (c) Streaming potential data for uncleaved mica basal planes in 1 mM KCl.

The following comparison between the action of ions of different charge on the mica basal plane is restricted to measurements at pH >5.5 and to samples that show strongly negative interfacial potentials. Figure 11a shows a comparison for results from SFA measurements. The cations are chosen such that no aqueous hydrolysis species occur, keeping the speciation simple and avoiding solution reactions that would also affect the pH. Clearly, the surface remains negative for the mono- and divalent salts. With the SFA, it was reported that measurements above 10 mM cation concentration resulted in too weak forces to measure. At very

high concentration, measurements show very interesting features that are related to hydration forces (triggered by the hydration shells of adsorbed cations). The divalent cations [here Ca, but the results are generic according to Pashley and Israelachvili for [73] alkaline earth elements, except Be, which strongly hydrolyzes and was not studied] generate less negative interfacial potentials than the monovalent cations. For the trivalent cation La, there is charge reversal. The surface turns positive at submillimolar concentrations. Figure 11b shows that the same kind of results has been independently obtained by zeta-potential measurements.

Figure 11c finally shows a direct comparison for the divalent cations (here Ca) in chloride solutions, now including also results from AFM-based experiments for which data on La^{3+} could not be found in our literature search. The comparison shows good agreement.

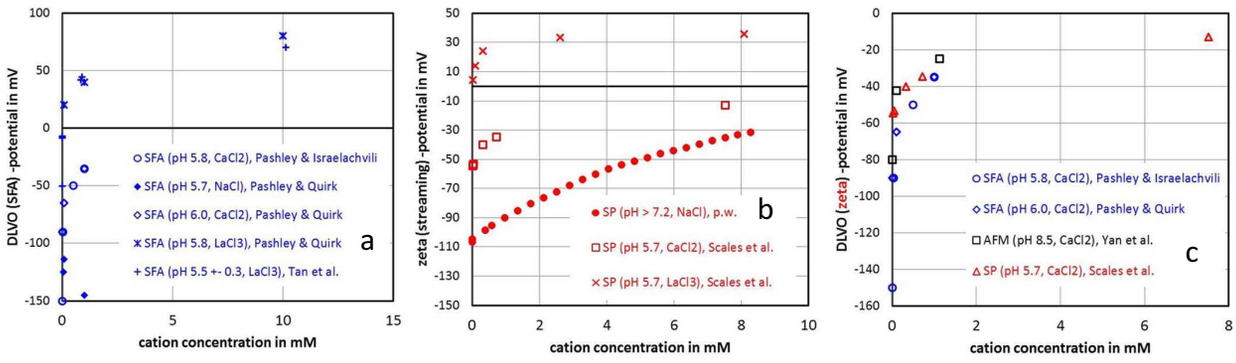

Figure 11. DLVO potentials from SFA experiments (a) and zeta-potentials from streaming potential measurements (b) of mica basal planes as a function of cation concentration at near-neutral pH for mono-, di-, and trivalent cations in chloride solutions. Data are from Pashley and Israelachvili [73], Pashley and Quirk [74], and Yan et al. [75] for Figure 11a and Scales et al. [68] for Figure 11b. (c) DLVO potentials from SFA and AFM experiments and zeta-potentials from streaming potential measurements of mica basal planes as a function of cation concentration at near-neutral pH for divalent cations in chloride solutions. Data are from Pashley and Israelachvili [73], Pashley and Quirk [74], Yan et al. [76], and Scales et al. [68].

The conclusion to be drawn from the above discussion of available data (note that we do not claim that the compilation of data is complete, nor do we claim that we have covered all available sources of measurements) is that tendencies are well retrieved for comparable samples and that even a quantitative agreement is probably achieved in particular for the divalent and trivalent cations at near-neutral pH.

The data also clearly prove that the valence of the cations strongly affects the interfacial potentials. This will be further discussed in Chapter 4 in the context of electrolyte titrations.

Despite the good agreement in some cases, caution is required when studying mica basal planes because widely varying results can be obtained depending on sample pre-treatment, mica origin (i.e. composition), and aging (i.e. duration of exposure to aqueous solution) as was shown shown in specific work devoted to these issues [77-79].

3.1.2. Basal plane versus edge faces

For mica, some data sets exist showing that the IEP of the edge plane is at pH approximately 8. Figure 12 shows such data for different runs. As pointed out before, the measurements on

http://dx.doi.org/10.5772/62082

the edge planes are difficult. However, the absolute values away from the IEP may strongly differ for data taken at different locations (thus varying in roughness in particular).

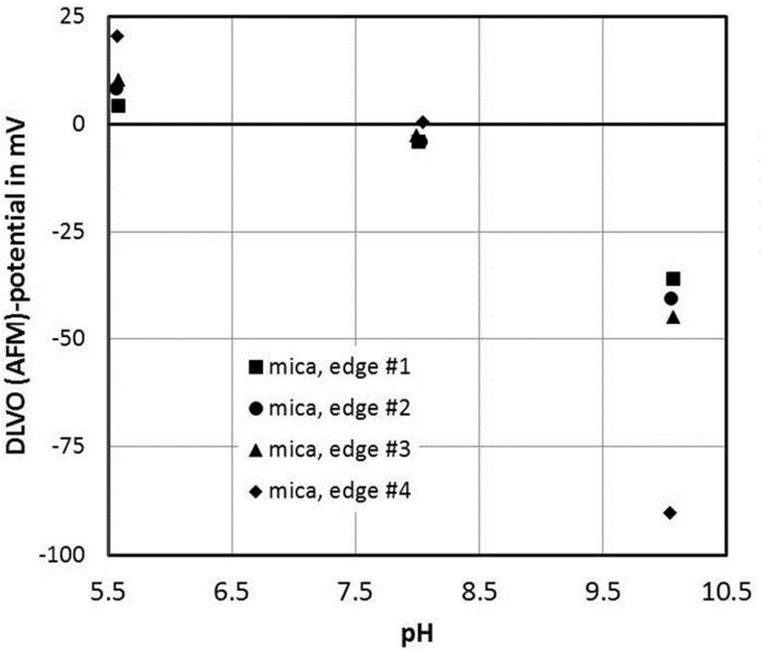

Figure 12. DLVO potentials from AFM experiments on mica edges as a function of salt concentration at pH 8.5 [60]; data sets 1 to 4 are taken at different spots and vary in surface roughness.

Figure 13 shows that even the action of divalent cations at pH 8.5 (i.e. where both basal plane and edge surfaces are intrinsically negative) will have very different effects. The data from Yan et al. show that [76], although the basal planes remain negative, the divalent cations are able to invert the charge on the edges. This clearly will generate anisotropy, and for the overall particle, it will require electrostatic (charge) regulation. It is not clear whether and how pH will be affected by such regulation.

3.2. Talc

Various data sets on talc are available from the literature. Zeta-potential measurements by Nalaskowski et al. [80] suggest IEPs for the edges and basal planes at pH approximately 3. The streaming potential measurements are in qualitative agreement with force distance curves by the same authors while showing distinct differences between the behavior of the edge and basal planes. The zeta-potential curves of the two planes are likewise not identical, so that the data appear self-consistent. These data sets, however, are in conflict with force measurements reported by Yan et al. [75] that are shown in Figure 14.

Figure 14a illustrates that the IEP of the basal plane is below pH 3 (i.e. at pH 5, the surface is still clearly negative), whereas that of the edges is at pH approximately 8. The origin of the differences is not clear. The latter study shows the anisotropy, which is further supported by data for divalent cations at pH 8.5 by [76] as shown in Figure 14b.

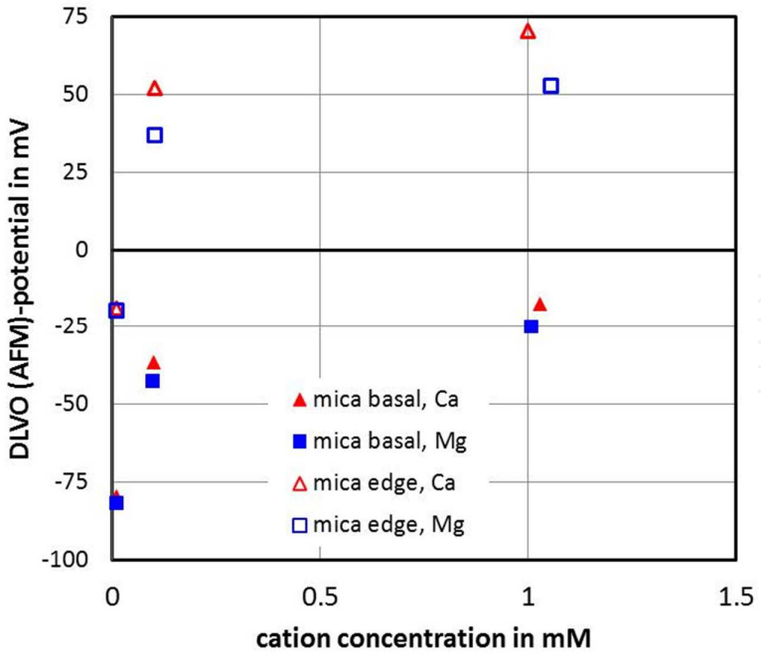

Figure 13. DLVO potentials from AFM experiments on mica basal plane and edge surfaces as a function of pH for 1 mM KCl solutions [76].

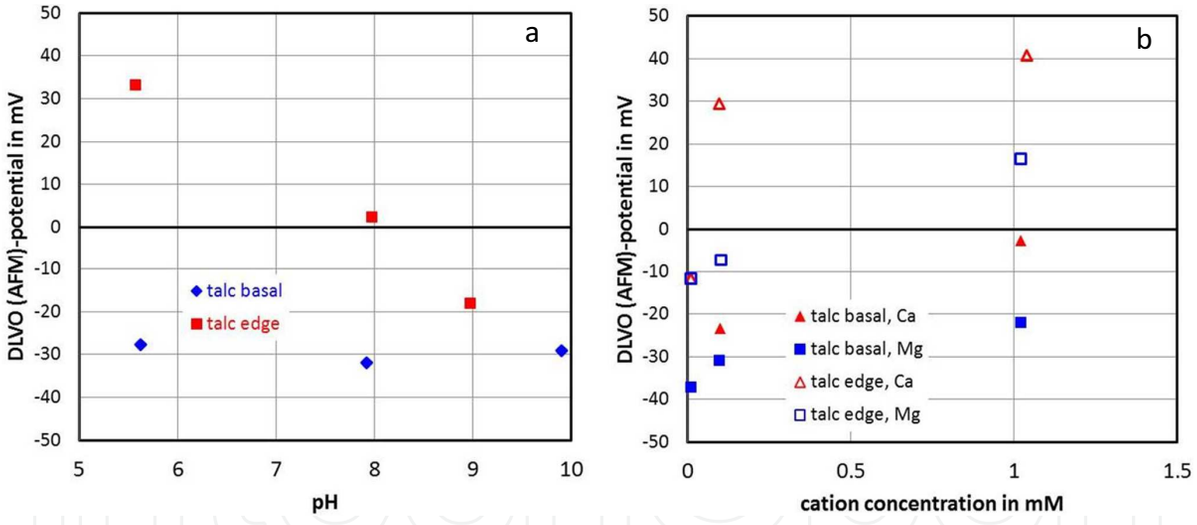

Figure 14. (a) DLVO potentials from AFM experiments on talc basal plane and edge surfaces as a function of pH for 1 mM KCl solutions [75]. (b) DLVO potentials from AFM experiments on talc basal plane and edge surfaces as a function of pH for 1 mM KCl solutions [76].

The results are similar to those obtained with mica shown in Figure 12. Again, the edge planes may change sign, whereas the basal plane remains negative. Similarly data for chlorite also exist and confirm the data sets discussed here, in general, and clearly exhibit anisotropy [70].

Overall, the examples shown in this part again suggest very complex situations when basal and edge surfaces are present simultaneously. Such situations are discussed in the following section, where first we discuss the amount of solid clay particles is buffering a suspension with

http://dx.doi.org/10.5772/62082

respect to pH yielding the overall point of zero net proton condition for the clay particles, whereupon, in the second step, the action of adding electrolyte to the buffered system can be investigated.

For the interpretation of such systems, assuming a full data set from force measurements or distinct measurements on specific planes were available, it would be very important to know whether there is a strong pH effect on the charge of a given plane or not. This is not always clear and may depend on many things as has been discussed in much detail for mica basal planes.

4. Surface properties of well-defined clay samples

As already discussed in the introduction, the macroscopic measurements that are applied to investigate the charging behavior have mainly involved electrokinetic methods, force measurements, and all kinds of titrations. The outcome of these measurements needs to be associated further with the properties of the EIL (electric interfacial layer). The relation of the measurements to the interfacial potentials has been described in detail elsewhere [12] and will only be shortly summarized here.

- Electrokinetic methods probe the overall charge within the so-called shear plane, which is at the head end of the immobile part of the EIL. In classical electrophoretic mobility experiments, where the velocity of a particle in an applied electric field is measured, the resulting interfacial potential (the so-called zeta-potentials) is the result of the interfacial species that are present within the immobile part (i.e. the particle and the water layer that is moving with the particle). The zeta-potential is unspecific in the sense that it gives the overall result from a multitude of processes that may occur on complex particles as would be the case for clays. Electrokinetic potentials of clay particles are typically negative over the full pH range investigated. The isoelectric point (IEP, at which the electrokinetic mobility is zero) is usually at low pH, sometimes not accessible to measurement. This result suggests that the negative, permanent charge is controlling the overall electrokinetic behavior of the clays. The application of the method has become standard and many experimental set-ups are available to determine the electrokinetic properties of particles.
- Titration methods may probe specific kinds of interactions. Potentiometric acid-base titrations [19, 81] will include all those interactions that involve reactions of the complete system with protons and hydroxide ions[8]. In the case of clays, it may include reactions with surface functional groups on basal planes, edge surfaces, ion-exchange sites as well as secondary phenomena (such as dissolution and subsequent reactions such as hydrolysis or complex formation), re-precipitation, or adsorption of species that were released during

8 This also includes dissolved carbon dioxide, which is a substantial complication due to the aqueous-phase reactions but also because carbon dioxide-related species can adsorb on surfaces. In all these reactions, protons are typically involved, which is why titrations are usually carried out in an inert atmosphere (such as purified argon). With natural clays, it is conceivable that calcite is present as a secondary mineral contained in a given sample, which makes the performance of reasonable acid-base titrations more or less senseless.

dissolution. It is probably impossible to disentangle contributions from the different phenomena in the analysis of a usual potentiometric acid-base titration. The method itself, though seemingly simple being an offspring of classical acid-base titrations, becomes quite complicated with surfaces. This is why often such titrations are carried out in the "fast" mode to limit the reactions to surface phenomena. However, if true equilibria involving dissolution and re-adsorption were to be considered, the approach would require substantial resources and analyses even for well-behaved oxide minerals.

- Mass titrations are a variant of potentiometric titrations [21, 23, 82]. They involve adding a known amount of solid to a solution of known composition and follow the evolution of the pH with increasing solid content. At a sufficient amount of solid in the system, the surface acid-base reactions buffer the system yielding the point of zero net proton charge for pure oxide systems. In such systems, the end point also coincides with the isoelectric point from electrokinetics. In the case of clays again, the situation is more complex.

- Yet, a further development of this technique is electrolyte titration [10]. From the effect of adding electrolyte to a surface buffered system on the resulting pH, the specific role of the electrolyte can be inferred. For well-behaved oxides, usually no effect is observed if inert electrolytes such as $NaClO_4$ are used. For clays as pointed out earlier, there are multiple effects of electrolyte ions that could play a role in such measurements. One would be the ion-exchange part, which could lead to reactions not related to classical acid-base equilibria, but yet they might cause interactions. For example, when a Ca-clay is interacting with high concentrations of a monovalent electrolyte, Ca will be released and the interactions of divalent ions in an electrostatic sense are much more pronounced than those of monovalent cations.

- Complications in these measurements arise from the suspension effect [83-86]. In the present case, this will be neglected as is the case in all other studies of this kind that we are aware of. Further problems occur in solutions of high electrolyte concentration, where specific interactions of electrolyte ions with the glass electrode perturb the measurements [87].

Potentiometric mass and electrolyte titrations were carried out to examine surface properties of artificial clay samples (Na-, Ca-, and Mg-montmorillonite). The use of such a synthetic sample has the advantage that no pre-treatment is required as is the case for natural samples where accessory minerals have to be extracted. A wide variety of salts was used and it was found that the different electrolytes had different effects on the end point of mass titrations. A synthetic Na-montmorillonite (SM) was used for the experimental work [88]. It has the formula $(Si_{3.8}Al_{0.2})/Al_{1.67}Mg_{0.33})O_{10}(OH_{1.9}F_{0.1})Na_{1.06}$ [88]. The external surface area was measured to be approximately 100 m^2/g (encompassing edges and basal plane surfaces), whereas the internal surface area was estimated to be approximately 700 m^2/g.

The clay was first used in its original Na-form. For additional experiments, it was transformed to Mg and Ca forms. For this purpose, the original Na-form was exposed to concentrated Mg or Ca solutions (0.1 mol/L) for 2 days to allow the ion exchange. After prolonged exposure to the concentrated Mg/Ca solutions, the transformed particles were separated from the supernatant by freeze-drying and reducing the surrounding pressure. For each sample, the proce-

http://dx.doi.org/10.5772/62082

dure was repeated three times, and we expect that most of the sodium was removed. The remainders of sodium would not interfere, because the starting conditions for the subsequent experiments were still the same, as all experiments with the three distinct forms were carried out from identical subsamples.

4.1. Potentiometric mass titrations of clay samples

Potentiometric mass titrations were used to determine the effect of solid content on the pH of suspension. According to theory [21-23, 82], the suspension pH will increase (or decrease) with solid content until a constant pH is finally reached that no longer depends on solid content. For samples without acid or base impurities, this plateau pH corresponds to the pH_{pznpc}. The surface of the particles is then buffering the pH of the suspension.

The known masses of the respective clay samples were added to an aqueous solution of pH_{in} in subsequent portions. After each addition and equilibration (at least 2 minutes under ultrasound and additional 10 minutes of stirring; the pH was found to remain constant after this procedure), the pH was recorded. The mass concentration beyond which the pH did not depend on solid mass content was approximately 35 g/dm^3. In these mass titrations, ionic strength (I_c=10^{-3} mol/dm^3; 10^{-2} mol/dm^3; 10^{-1} mol/dm^3) was controlled by the addition of electrolyte (NaCl in the case of Na-form and $CaCl_2$ in the case of Ca-form of montmorillonite).

The results from the potentiometric mass titrations were used to determine the effect of ionic strength on pH_{pznpc} of the clays and to evaluate the proton-related surface charge densities.

Figures 15 and 16 show the results from mass titrations for the clay in its Na and Ca forms, respectively. Data for various starting values of pH and different electrolyte concentrations were obtained. The end points from the different starting points clearly converge with increasing solid concentration for a given ionic strength. With increasing salt content, it appears that the plateau can be reached at lower mass contents. For metal oxides [22], it had been observed that the plateau would be reached at lower mass concentration for higher ionic strength and if initial pH_{in} is close to pH_{pznpc}. One reason for this difference could be that the slope of the pH(γ) function corresponds to the surface charge density, which is steeper for the higher ionic strength. Accordingly, proton-related surface charge density functions $\sigma_{0,H+}$(pH) for clays are shifted with salt content (without any cross-point) and are nearly parallel [89]. The resulting end points (obtained or interpolated) are 7.1±0.1 (for 10^{-3} mol/dm^3 NaCl), 6.9±0.1 (for 10^{-2} mol/dm^3 NaCl), and 6.6±0.1 (for 10^{-1} mol/dm^3 NaCl). Despite the experimental error, there is a clear trend for the end points to decrease with increasing ionic strength. This is expected based on the reported parallel shift of proton surface charge data as a function of ionic strength. For the Ca-form, as for the sodium form, the average plateau pH decreases with increasing salt content.

From the mass titration data, the specific surface charge densities (related to proton and hydroxide adsorption) can be calculated [22, 23]. The advantage of this method, compared to traditional acid-base potentiometric titrations, is that experiments can be performed at one ionic strength and also at very low electrolyte concentrations. Moreover, a comparison of the dispersion with blank titration is not required. The surface charge of an oxide in an aqueous

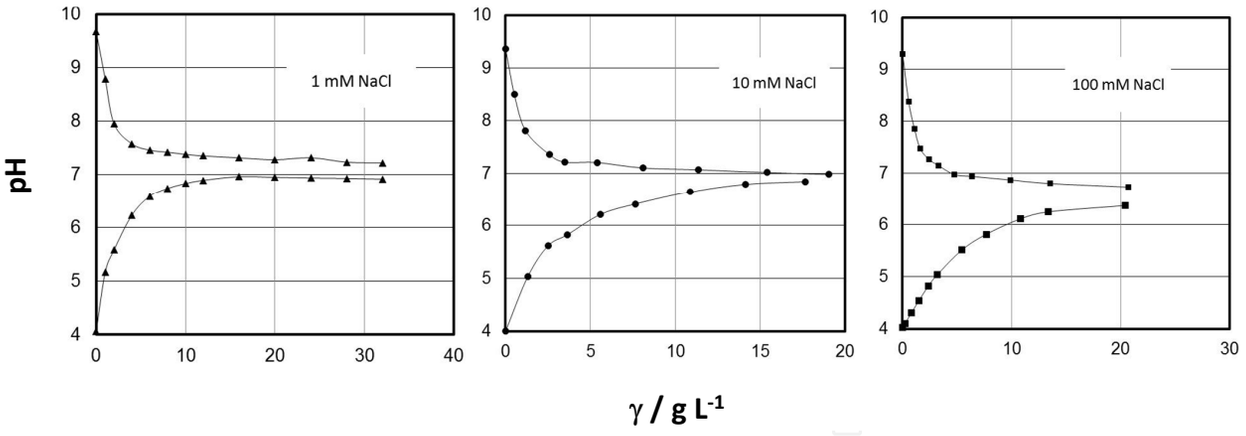

Figure 15. Potentiometric mass titrations of ACF2944 (Na-form) at different ionic strengths: I_c (mol/dm^3): 0.001 (▲), 0.01 (●), and 0.1 (■) NaCl; t=20°C. Shown are the values of the end points of mass titrations (pH_{pznpc}) for the synthetic clay in its Na-form.

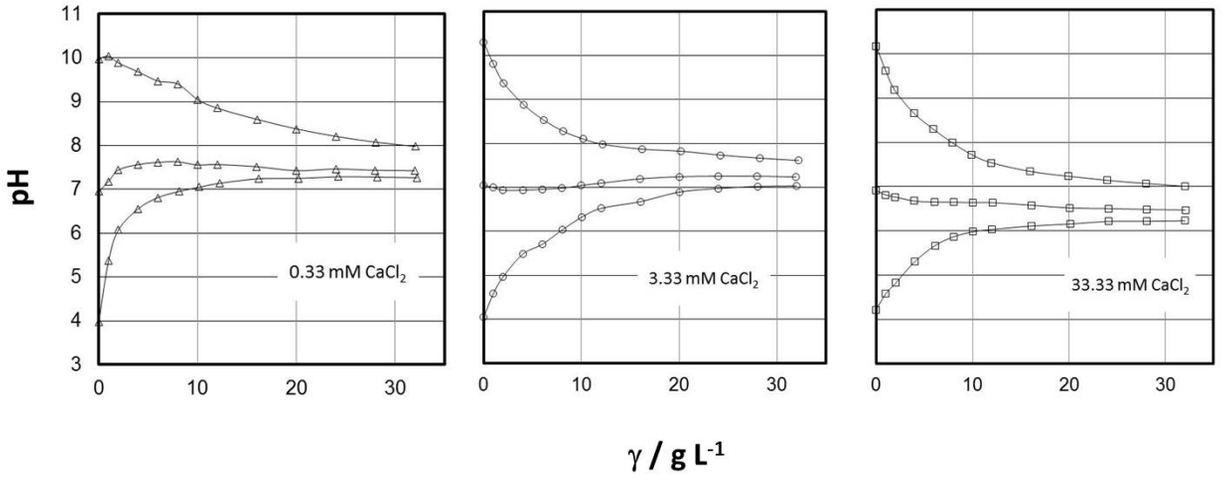

Figure 16. Potentiometric mass titrations of ACF2944 (Ca-form) at different ionic strengths: I_c (mol/dm^3): 0.001 (Δ), 0.01 (○), and 0.1 (□). Ionic strength was controlled by $CaCl_2$; t=20°C.

environment is the result of surface reactions (protonation, de-protonation, and counter-ion association). In the course of mass titration, when a solid metal oxide powder is added to an aqueous electrolyte solution, the amounts (and concentrations) of H^+ and OH^- ions in the bulk of the solution are changing due to surface reactions but also due to the possible neutralization of H^+ and OH^- ions in the bulk of the solutions. In the case of a pure sample (without acid or base impurities), the surface charge density in the 0-plane equals [23]:

$$\sigma_{0,H^+} = -\frac{F}{\gamma}\frac{c^\circ}{\overline{y}_\pm}\left(10^{-pH_\gamma} - 10^{-pH_{in}} - 10^{pH_\gamma - pK_W^\circ} + 10^{pH_{in} - pK_W^\circ}\right) \quad (1)$$

http://dx.doi.org/10.5772/62082

where γ is the mass concentration of solid particles, $\bar{y}_{\pm}$ is the mean activity coefficient calculated from the Debye-Hückel equation, and K_W° is the thermodynamic equilibrium constant of water ionization. Furthermore, pH_{in} is the initial pH, pH_{γ} is the pH of suspension at mass concentration γ, c° is the standard concentration (1 mol/dm^3), and F is the Faraday constant. To cover both acidic and basic pH ranges, at least two experiments should be performed, one with low and another with high initial pH.

Figure 17 presents the proton-related surface charge densities obtained from the potentiometric mass titration data according to a previously described procedure [23] for different concentrations of NaCl and $CaCl_2$. As expected, a CIP of titration curves as a function of electrolyte concentration is not obtained. The PZNPC is shifted towards lower pH values with increasing electrolyte concentration. For the range between 10^{-3} and 10^{-1} mol/dm^3 concentration of NaCl, we obtain, on average, a difference of ΔpH_{pznpc}=0.9 for $CaCl_2$.

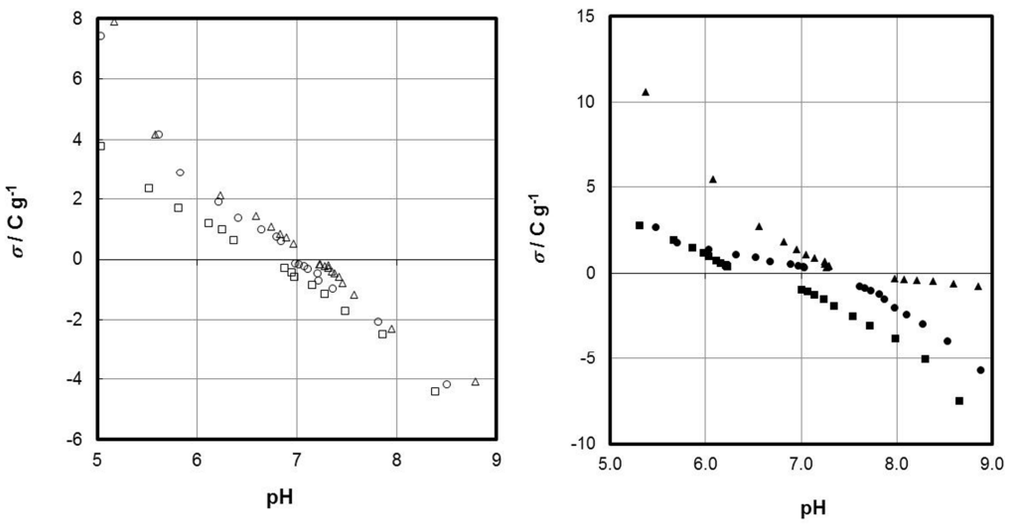

Figure 17. (a) Surface charge density of ACF2944 (Na-form) (calculated from mass titration data shown on Figure 15) at different ionic strength: I_c (mol/dm^3): 0.001 (Δ), 0.01 (○), and 0.1 (□); NaCl; t=20°C. (b) Surface charge density of ACF2944 (Ca-form) (calculated from mass titration data shown on Figure 16) at different ionic strength: I_c (mol/dm^3): 0.00033 (▲),0.0033 (●), and 0.033 (■). Ionic strength was controlled by $CaCl_2$; t=20°C.

4.2. Potentiometric electrolyte concentrations of clay samples

In the potentiometric electrolyte titrations, an initial clay suspension was prepared by adding the amount of powder to pure water that is sufficient to obtain the plateau pH. The standard value γ≈35 g/dm^3 had been previously determined in the mass titrations (see above). Subsequently, known aliquots of dry salt [NaCl, CsCl, $CaCl_2$, $LiNO_3$, $NaNO_3$, or $Ca(NO_3]_2$] were added to the initial dispersion to scan a range of salt concentrations from 10^{-5} to 0.5 mol/dm^3. The pH values of the dispersion obtained after each salt addition were measured after equilibration (at least 2 minutes under ultrasound and 10 minutes of stirring).

The results from electrolyte titrations results from electrolyte titrations for this sample are shown are shown in Figure 18 for three salts (NaCl, CsCl, and $LiNO_3$) at a mass concentration

of 35 g/l Na-montmorillonite. In Figure 18, we also include the independent results from the direct mass titrations with the experimental errors based on the end-point values shown in Figure 16. A satisfactory agreement is found considering that the solid concentrations in the two experiments are not identical. This shows that the procedure is reliable. The lower solid concentrations in the continuous (pH) titrations tend to generate stronger effects based on the results in Figure 15a. The results of the electrolyte and mass titrations show that the effect of salt concentration is weak or absent at salt concentrations below approximately 1 mM. Above this value, however, a significant decrease of the mass titration end-points occurs in the electrolyte titrations for all salts tested.

A comparison between the different salts suggests that CsCl has a much stronger effect than NaCl, in agreement with the known strong affinity of Cs for clays [90, 91]. $LiNO_3$ has the weakest effect among the salts shown. The data sets indicate that different cations will have different effects on proton uptake on this clay, an observation that needs to be taken into account in comprehensive models to describe the charging of clays via ion-specific parameters.

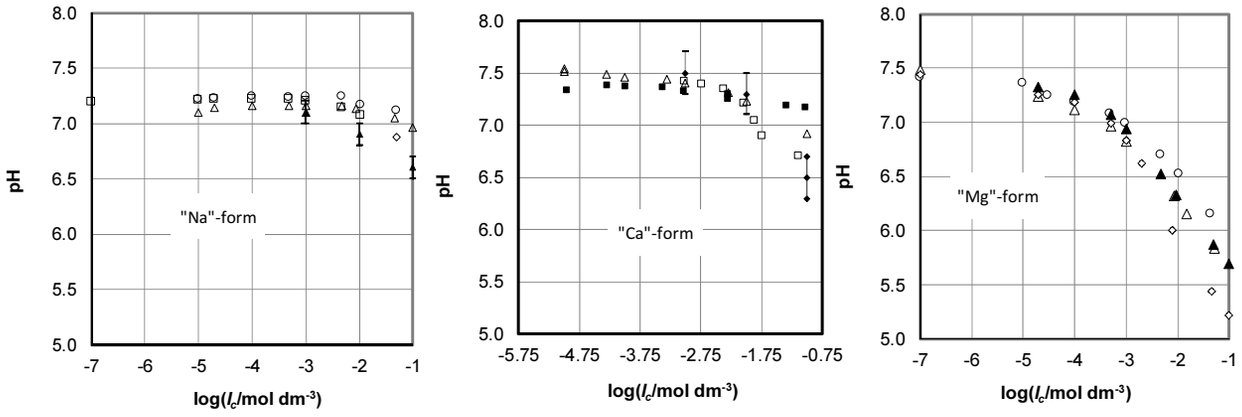

Figure 18. Potentiometric electrolyte titrations of ACF2944. (a) Na-form with NaCl (Δ), $LiNO_3$ (○), and CsCl (◇) and end points of mass titration (▲ with error bars); (b) Ca-form with NaCl (Δ), $Ca(NO_3)_2$ (■), and $CaCl_2$ (□) and end points of mass titration (◆ with error bars); and (c) Mg-form with NaCl (Δ), $NaNO_3$ (▲), $LiNO_3$ (○), and CsCl (◇).

Figure 18 shows the results of the electrolyte titrations with Ca-montmorillonite. First, it becomes apparent that the variation of the pH values is much more pronounced than in the case of the Na-montmorillonite. The drop in pH again starts at approximately 1 mM concentration as for the Na-clay. The sequence is somewhat surprising in the sense that $Ca(NO_3)_2$ has a much weaker effect than does $CaCl_2$, given that the cation was to be the most relevant compound for the negatively charged surface.

For the Mg-form (Figure 18c), the effect of the electrolyte ions on the mass titration end-points starts at significantly lower concentration compared to the Na-form. The effect appears to be unspecific, however, up to approximately 1 mM concentration. Unlike in the previous example for Ca salts on Ca-montmorillonite, we did not observe a noticeable difference between NaCl and $NaNO_3$ systems, indicating that the nature of the anions tested in this case does not affect the results in a significant way. The order in which the cations affect the results is the same as for the Na-form of the clay, but the extent of the changes is much more pronounced for the Mg-form.

http://dx.doi.org/10.5772/62082

5. Reconciliation of results

The literature survey has shown that the understanding of clay surfaces in electrolyte solutions still has some space to improve. One important question is to what extent the aging of samples should be studied. Even if the aging steps and their consequences are not well studied and probably difficult to understand due to the complexity and the interdependencies of the process involved, natural samples will have undergone such aging. Simple aging in water can have significant effects on the interfacial potentials of relevant minerals as has been shown in the preceding text. Aging will make the surfaces more complex with adsorbed ions, and surely it will make them different from the ideal surfaces that can be obtained experimentally for sufficiently small times and conditions that would conserve the ideality and from those that have been used in computer codes to extract pK values.

Thus, a dual procedure is required to come to a full understanding:

- Comprehensive studies on the ideal systems involving the full monitoring of all potentially important features (solution composition, surface states, etc.) to gain insight in processes.
- Studies on the aging process and on aged samples to allow the transfer of the fundamental studies to the natural samples.

The wide range of reported values for isoelectric points or points of zero (net proton) charge of clay samples have to be considered with care in light of the aging processes and the potential effects of exposure to low or high pH conditions. This has been discussed in some detail for mica. We could add here that titrations of cleaved mica [92] have resulted in a pK value of 2.9, in strong contrast with the AFM data shown in Figure 12 for mica edges (always taking the general view that the basal plane is not proton sensitive and that consequently the proton reactions occur at the edges). As stated in the discussions about the techniques, such proton titrations will yield relative values, which may be overshadowed by permanent charge. The authors of the latter paper actually do conclude that the charge from deprotonation reactions is small compared to the permanent charge. In terms of published parameter, this all generates yet another set of contradictions given that the pK based on the AFM data would be 8 [60] and that the zeta-potential of freshly cleaved basal planes is pH sensitive as apparent from Figure 9a in particular for the low pH. Thus, the reported pK value from titrations could also stem from proton reactions at the basal plane. These could either occur at surface functional groups or be due to unconventional reactions of hydroxide ions on smooth surfaces.

We may continue by comparing the results of anions on the mica basal plane to the unexpected observations discussed in the electrolyte titrations in the previous section. Figure 19 illustrates that such effects are retrieved on the mica basal plane as well.

Both for monovalent Li solutions and for divalent Ca solutions, there is a difference between chloride and nitrate solutions. However, the effects are not the same: whereas, in the Li case, there is a strong decrease in the DLVO potential (an increase in absolute potential), in the Ca case, the opposite occurs. A study on ion-specific effects on sapphire-c has shown similar effects of nitrate versus chloride [62]. The co-adsorption of chloride as postulated for the

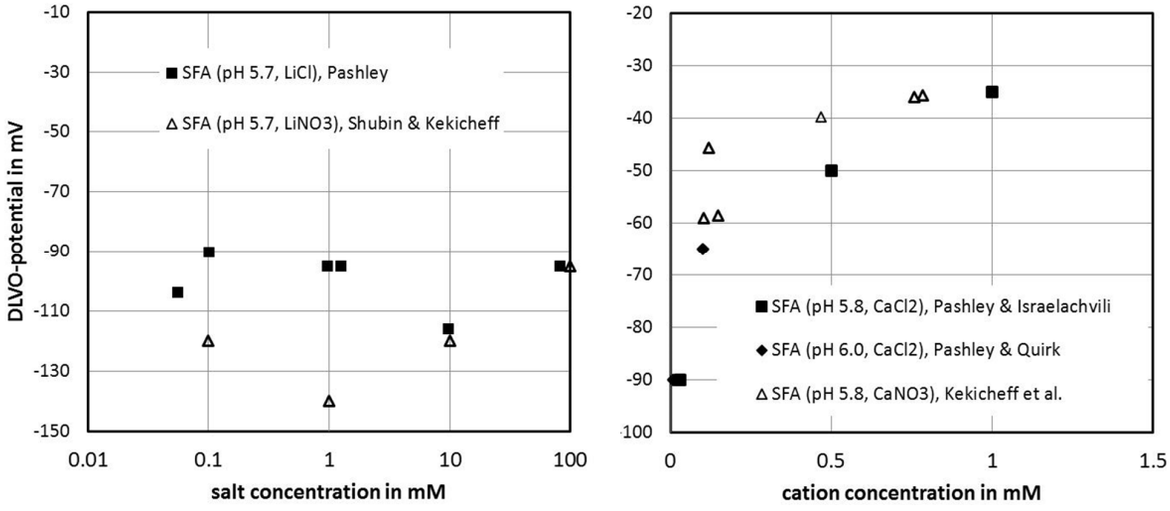

Figure 19. DLVO potentials of mica basal planes in chloride versus nitrate solutions. Left: Li solutions, data are from Pashley [67] and Shubin and Kekicheff [93]. Right: Ca solutions, data are from Pashley and Israelachvili [73], Pashley and Quirk [74], and Kekicheff et al. [94].

gibbsite basal plane [40] in Ca solutions could also explain the observation on sapphire-c. The pH dependence of and thus potential effects on the solution pH caused by such correlative interactions is not known at all but might explain the effect observed in the electrolyte titrations shown in Figure 18. The larger effect of the chloride would imply a stronger release of protons or co-adsorption of hydroxide ions in chloride solutions compared to nitrate solutions. This would keep the DLVO potentials higher in absolute values in the chloride systems, which is observed for the mica case (Figure 19) and concurs with the observations on sapphire-c as well. Such comparisons generate circumstantial evidence for the actions of hydroxide ions (or protons). The combining issue could be flat surfaces (for mica and sapphire-c, this is obvious; for the clay particles, it would mean that the reactions are happening on the basal planes). However, it would need to be a collective action of chloride and hydroxide ions (or protons) to explain the overall effect (i.e. causing changes in pH and the interfacial potential in the observed directions). It can be seen that, for the monovalent Li system on mica, this explanation cannot be sustained. However, the trend for the chloride system is also present, whereas the disagreeing observation for nitrate occurs in the very low concentration range.

To address the aging problem, we draw attention to a completely different field of research. In a recent study on mica as an active ice nucleation clay mineral, the structuring of water molecules at the surface of mica upon cooling using second harmonic generation (SHG) spectroscopy was measured [95]. Freshly cleaved mica induced the local ordering of the first water layer in contact with the surface, which was termed pre-activation of ice nucleation. This local ordering was recorded as the enhancement of the SHG upon cooling. Interestingly, small variations were observed from run to run for freshly cleaved samples. This is similar to what was discussed for mica in the previous sections. In the ice nucleation study, samples that were kept in contact with water for a longer time clearly exhibited an aging effect. Figure 20 reports additional results that only focus on the aging effect on the water/mica surface interaction.

http://dx.doi.org/10.5772/62082

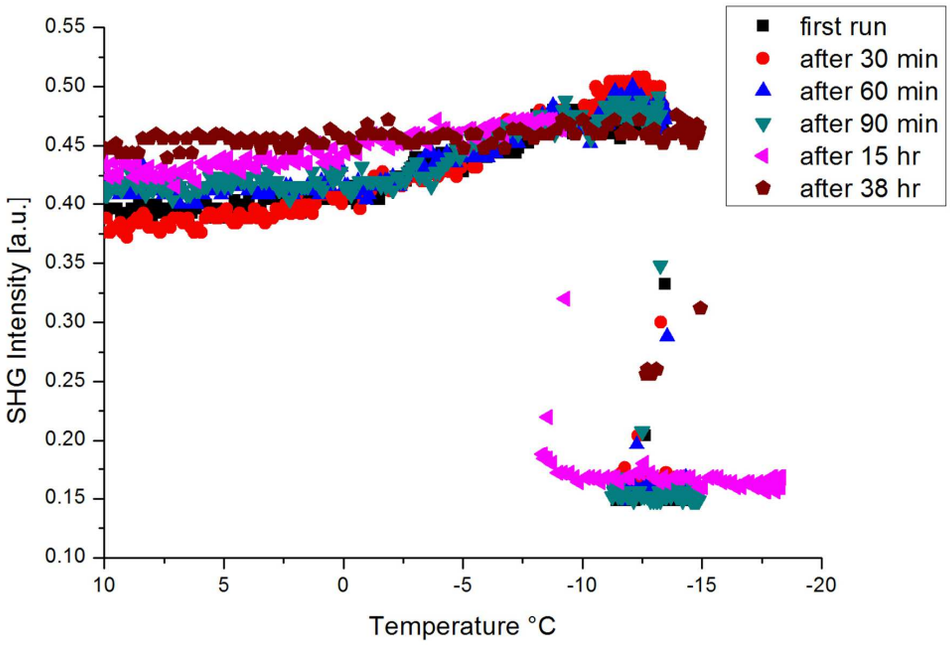

Figure 20. Second harmonic generation signals recorded in ice nucleation studies on a mica sample at different times.

Figure 20 shows the SHG signal at water-mica interface for the same sample after different aging periods. Measurements done within a few hours after the cleavage showed water ordering under cooling, and small variations were observed at high temperatures. Measurements carried out after 15 hours showed weaker ordering with cooling. Measurements carried out after 38 hours showed an almost temperature-independent signal in the liquid phase. In all measurements, the level of signal was different, particularly at high temperatures. For both the aqueous electrolyte mica interface and the ice nucleation study, the question will be what is the relevant surface to study. For most environmental applications, it will be an aged surface, although probably for fundamental studies aimed at process understanding fresh surfaces that are well defined should be preferable.

The anisotropy of the clay particles has relevance in many respects. The aggregation of the particles is highly affected by it as is the migration of clay particles. The spillover effects are complex and only few efforts have been dedicated to this issue. The effects become even more complex at points where more than just two surface planes meet (for example, two different edge planes and two different basal planes could be very close on kaolinite). The currently available experimental observations on the clay edges are still confusing in the sense that, for kaolinite, the edge surface data suggest a low point of zero charge contrary to expectations based on a previous experimental work. Interestingly, theoretical work does show the pK value for aluminols on kaolinite to be lower than in other cases [i.e. 5.7 for kaolinite versus 8.3 for montmorillonite [56] or 7.6 for pyrophillite [47]]. Calculations also show that the pK values may differ between these extremes for a given solid depending on which edge surface is considered [96]. For talc and mica instead, the experimental points of zero charge (isoelectric points) determined for edges are in the expected range and in reasonable agreement with predicted pK values from advanced theoretical work [47, 56, 96] but disagree, for example,

with the above-mentioned titrations [92]. One has to keep in mind that the titrations (that also have been used in the cited theoretical work for comparison) may be misleading. Titrations yield relative changes, whereas the models used to extract pK values in surface complexation models will require absolute values (of charge of protons adsorbed or whatever quantity is used to fit surface complexation parameters). These absolute values are typically not available for clays. Furthermore, the shape of the titration curve or the relative charges versus pH cannot help because electrostatic factors may shift apparent pK values by many pH units from the intrinsic values (i.e. at zero surface potential).

As a consequence, it is probably necessary to improve the experimental data basis to come to more profound conclusions. In particular, a study on different clay edge surfaces could be important, but this is a significant experimental challenge. If the preparative issue was solved, one could test spillover effects at points where two edge surfaces meet for example. For the calculation work, it could turn out to be useful to report estimates for site densities of the sites that were studied as well as formal charges of the surface species. Furthermore, for comparison with experimental data and to scan the range of reported points of zero charge, it might turn out to be useful to explore the role of adsorbed ions (such as aluminum). It is noteworthy that some steps into such a direction have been taken by including potential composite ions such as Mg, Fe, or others in the calculations [56, 97].

Overall, a comprehensive study involving a multitude of experimental and theoretical approaches, with close collaboration to exactly mimic the experimental surfaces in the calculations, would be highly beneficial. This conclusion has also been drawn for seemingly simpler systems such as metal oxide surfaces.

Although the advances in the detailed understanding and the possibilities with modern experimental and computational techniques are breathtaking, much can be expected to surprise us in the future when taking an even closer look at mineral-electrolyte solution interfaces.

Acknowledgements

The authors express their gratitude to Dr. Igor Siretanu (University of Enschede) for providing the potentials from the force measurements that were originally published in terms of charge densities. Professor Thomas Leisner (Karlsruhe Institute of Technology, IMK-AAF) is gratefully acknowledged for the support with the SHG study.

Author details

Tajana Preocanin[1], Ahmed Abdelmonem[2], Gilles Montavon[3] and Johannes Luetzenkirchen[4*]

*Address all correspondence to: johannes@ine.fzk.de

http://dx.doi.org/10.5772/62082

1 Laboratory of Physical Chemistry, Department of Chemistry, Faculty of Science, University of Zagreb, Zagreb, Croatia

2 Institute of Meteorology and Climate Research-Atmospheric Aerosol Research (IMK-AAF), Karlsruhe Institute of Technology (KIT), Germany

3 Subatech, UMR 6457 (Ecole des Mines/CNRS-IN_2P_3/Nantes University), Nantes, France

4 Institut für Nukleare Entsorgung (INE), Karlsruhe Institute of Technology (KIT), Germany

References

[1] Lützenkirchen J. Determination of points of zero charge of minerals, experimental and computational approaches. Current Topics in Colloid & Interface Science. 2002;5:125 - 39.

[2] Sposito G. On points of zero charge. Environmental Science & Technology. [Article]. 1998 Oct;32(19):2815-9.

[3] Sposito G. On Points of Zero Charge. Environmental Science & Technology. 1999 1999/01/01;33(1):208-.

[4] Kosmulski M. Chemical Properties of Material Surfaces: CRC Press; 2001.

[5] Kosmulski M. Surface Charging and Points of Zero Charge: CRC Press; 2009.

[6] Venema P, Hiemstra T, Weidler PG, van Riemsdijk WH. Intrinsic Proton Affinity of Reactive Surface Groups of Metal (Hydr)oxides: Application to Iron (Hydr)oxides. Journal of Colloid and Interface Science. 1998;198(2):282-95.

[7] Hiemstra T, Van Riemsdijk WH. On the relationship between charge distribution, surface hydration, and the structure of the interface of metal hydroxides. Journal of Colloid and Interface Science. 2006;301(1):1-18.

[8] Rahnemaie R, Hiemstra T, van Riemsdijk WH. A new surface structural approach to ion adsorption: Tracing the location of electrolyte ions. Journal of Colloid and Interface Science. 2006;293(2):312-21.

[9] Bradbury MH, Baeyens B. Sorption modelling on illite Part I: Titration measurements and the sorption of Ni, Co, Eu and Sn. Geochimica et Cosmochimica Acta. 2009;73(4): 990-1003.

[10] Lützenkirchen J, Preočanin T, Bauer A, Metz V, Sjöberg S. Net surface proton excess of smectites obtained from a combination of potentiometric acid–base, mass and electrolyte titrations. Colloids and Surfaces A: Physicochemical and Engineering Aspects. 2012;412:11-9.

[11] Bradbury MH, Baeyens B. Sorption of Eu on Na- and Ca-montmorillonites: experimental investigations and modelling with cation exchange and surface complexation. Geochimica et Cosmochimica Acta. 2002;66(13):2325-34.

[12] Kallay N, Preočanin T, Kovačević D, Lützenkirchen J, Chibowski E. Electrostatic potentials at solid/liquid interfaces. Croatica chemica acta. 2010;83(3):357-70.

[13] Lützenkirchen J. Summary of studies on (ad) sorption as a "well-established" process within FUNMIG activities. Applied Geochemistry. 2012;27(2):427-43.

[14] Gan Y, Franks GV. Charging behavior of the gibbsite basal (001) surface in NaCl solution investigated by AFM colloidal probe technique. Langmuir. 2006;22(14):6087-92.

[15] Liu X, Cheng J, Sprik M, Lu X, Wang R. Understanding surface acidity of gibbsite with first principles molecular dynamics simulations. Geochimica et Cosmochimica Acta. 2013;120:487-95.

[16] Hiemstra T, Yong H, Van Riemsdijk W. Interfacial charging phenomena of aluminum (hydr) oxides. Langmuir. 1999;15(18):5942-55.

[17] Lützenkirchen J, Abdelmonem A, Weerasooriya R, Heberling F, Metz V, Marsac R. Adsorption of dissolved aluminum on sapphire-c and kaolinite: implications for points of zero charge of clay minerals. Geochemical transactions. 2014;15(1):9.

[18] Lutzenkirchen J, Zimmermann R, Preocanin T, Filby A, Kupcik T, Kuttner D, et al. An attempt to explain bimodal behaviour of the sapphire c-plane electrolyte interface. Adv Colloid Interfac. 2010 Jun 14;157(1-2):61-74.

[19] Lützenkirchen J, Preočanin T, Kovačević D, Tomišić V, Lövgren L, Kallay N. Potentiometric titrations as a tool for surface charge determination. Croatica chemica acta. 2012;85(4):391-417.

[20] Delgado AV, Gonzalez-Caballero F, Hunter RJ, Koopal LK, Lyklema J. Measurement and interpretation of electrokinetic phenomena. Journal of Colloid and Interface Science. [Article; Proceedings Paper]. 2007 May;309(2):194-224.

[21] Noh JS, Schwarz JA. Estimation of the point of zero charge of simple oxides by mass titration. Journal of Colloid and Interface Science. 1989;130(1):157-64.

[22] Preocanin T, Kallay N. Point of zero charge and surface charge density of TiO2 in aqueous electrolyte solution as obtained by potentiometric mass titration. Croatica chemica acta. 2006 Mar;79(1):95-106.

[23] Preočanin T, Kallay N. Application of» Mass Titration «to Determination of Surface Charge of Metal Oxides. Croatica chemica acta. 1998;71(4):1117-25.

[24] Trasatti S, Doubova LM. Crystal-face specificity of electrical double-layer parameters at metal/solution interfaces. Journal of the Chemical Society, Faraday Transactions. [10.1039/FT9959103311]. 1995;91(19):3311-25.

[25] Hiemstra T, De Wit JCM, Van Riemsdijk WH. Multisite proton adsorption modeling at the solid/solution interface of (hydr)oxides: A new approach: II. Application to various important (hydr)oxides. Journal of Colloid and Interface Science. 1989;133(1): 105-17.

[26] Lützenkirchen J, Behra P. A new approach for modelling potential effects in cation adsorption onto binary (hydr) oxides. Journal of contaminant hydrology. 1997;26(1): 257-68.

[27] Secor RB, Radke CJ. Spillover of the diffuse double layer on montmorillonite particles. Journal of Colloid and Interface Science. 1985;103(1):237-44.

[28] Chang F-RC, Sposito G. The Electrical Double Layer of a Disk-Shaped Clay Mineral Particle: Effects of Electrolyte Properties and Surface Charge Density. Journal of Colloid and Interface Science. 1996;178(2):555-64.

[29] Bourg IC, Sposito G, Bourg ACM. Modeling the acid–base surface chemistry of montmorillonite. Journal of Colloid and Interface Science. 2007;312(2):297-310.

[30] Tournassat C, Grangeon S, Leroy P, Giffaut E. Modeling Specific pH Dependent Sorption of Divalent Metals on Montmorillonite Surfaces. A Review of Pitfalls, Recent Achievements and Current Challenges. Am J Sci. [Article]. 2013 May;313(5): 395-451.

[31] Lützenkirchen J, Preočanin T, Stipić F, Heberling F, Rosenqvist J, Kallay N. Surface potential at the hematite (001) crystal plane in aqueous environments and the effects of prolonged aging in water. Geochimica et Cosmochimica Acta. 2013;120:479-86.

[32] Yanina SV, Rosso KM. Linked Reactivity at Mineral-Water Interfaces Through Bulk Crystal Conduction. Science. 2008;320(5873):218-22.

[33] Luetzenkirchen J, Zimmermann R, Preocanin T, Filby A, Kupcik T, Kuettner D, et al. An attempt to explain bimodal behaviour of the sapphire c-plane electrolyte interface. Advances in Colloid and Interface Science. 2010 Jun 14;157(1-2):61-74.

[34] Kallay N, Preocanin T, Selmani A, Kovacevic D, Luetzenkirchen J, Nakahara H, et al. Thermodynamic Model of Charging the Gas/Water Interface. Journal of Physical Chemistry C. 2015 Jan 15;119(2):997-1007.

[35] Anderson JL. Effect of Nonuniform Zeta Potential on Particle Movement in Electric-Fields. Journal of Colloid and Interface Science. 1985 1985;105(1):45-54.

[36] Franks GV, Gan Y. Charging behavior at the alumina–water interface and implications for ceramic processing. Journal of the American Ceramic Society. 2007;90(11): 3373-88.

[37] Catalano JG. Weak interfacial water ordering on isostructural hematite and corundum (0 0 1) surfaces. Geochimica et Cosmochimica Acta. 2011;75(8):2062-71.

[38] Park C, Fenter PA, Nagy KL, Sturchio NC. Hydration and distribution of ions at the mica-water interface. Physical review letters. 2006;97(1):016101.

[39] Schlegel ML, Nagy KL, Fenter P, Cheng L, Sturchio NC, Jacobsen SD. Cation sorption on the muscovite (001) surface in chloride solutions using high-resolution X-ray reflectivity. Geochimica et Cosmochimica Acta. 2006;70(14):3549-65.

[40] Siretanu I, Ebeling D, Andersson MP, Stipp SLS, Philipse A, Stuart MC, et al. Direct observation of ionic structure at solid-liquid interfaces: a deep look into the Stern Layer. Sci Rep. [Article]. 2014;4.

[41] Gupta V, Hampton MA, Stokes JR, Nguyen AV, Miller JD. Particle interactions in kaolinite suspensions and corresponding aggregate structures. Journal of Colloid and Interface Science. 2011;359(1):95-103.

[42] Gupta V, Miller JD. Surface force measurements at the basal planes of ordered kaolinite particles. Journal of Colloid and Interface Science. 2010;344(2):362-71.

[43] Yin X, Miller J. Wettability of kaolinite basal planes based on surface force measurements using atomic force microscopy. Minerals and Metallurgical Processing. 2012;29(1):13-9.

[44] Liu J, Sandaklie-Nikolova L, Wang X, Miller JD. Surface force measurements at kaolinite edge surfaces using atomic force microscopy. Journal of Colloid and Interface Science. 2014;420:35-40.

[45] Williams DJA, Williams KP. Electrophoresis and Zeta Potential of Kaolinite. Journal of Colloid and Interface Science. 1978 1978;65(1):79-87.

[46] Zhou ZH, Gunter WD. The Nature of the Surface-Charge of Kaolinite. Clay Clay Min. 1992 Jun;40(3):365-8.

[47] Tazi S, Rotenberg B, Salanne M, Sprik M, Sulpizi M. Absolute acidity of clay edge sites from ab-initio simulations. Geochimica et Cosmochimica Acta. [Article]. 2012 Oct;94:1-11.

[48] Miller JD, Nalaskowski J, Abdul B, Du H. Surface characteristics of kaolinite and other selected two layer silicate minerals. The Canadian Journal of Chemical Engineering. 2007;85(5):617-24.

[49] Alagha L, Wang S, Yan L, Xu Z, Masliyah J. Probing Adsorption of Polyacrylamide-Based Polymers on Anisotropic Basal Planes of Kaolinite Using Quartz Crystal Microbalance. Langmuir. 2013 2013/03/26;29(12):3989-98.

[50] Gupta V. Surface charge features of kaolinite particles and their interactions: The University of Utah; 2011.

[51] Liu XD, Cheng J, Sprik M, Lu XC, Wang RC. Understanding surface acidity of gibbsite with first principles molecular dynamics simulations. Geochimica et Cosmochimica Acta. [Article]. 2013 Nov;120:487-95.

[52] Adekola F, Fedoroff M, Geckeis H, Kupcik T, Lefevre G, Lutzenkirchen J, et al. Characterization of acid-base properties of two gibbsite samples in the context of literature results. J Colloid Interf Sci. 2011 Feb 1;354(1):306-17.

[53] Rosenqvist J, Persson P, Sjoberg S. Protonation and charging of nanosized gibbsite (alpha-Al(OH)(3)) particles in aqueous suspension. Langmuir. [Article]. 2002 Jun; 18(12):4598-604.

[54] Lutzenkirchen J, Kupcik T, Fuss M, Walther C, Sarpola A, Sundman O. Adsorption of Al-13-Keggin clusters to sapphire c-plane single crystals: Kinetic observations by streaming current measurements. Appl Surf Sci. 2010 Jun 15;256(17):5406-11.

[55] Lutzenkirchen J, Marsac R, Casey WH, Furrer G, Kupcik T, Lindqvist-Reis P. The Effect of Monovalent Electrolytes on the Deprotonation of MAl12 Keggin Ions. Aquat Geochem. 2015 Jul;21(2-4):81-97.

[56] Liu XD, Lu XC, Sprik M, Cheng J, Meijer EJ, Wang RC. Acidity of edge surface sites of montmorillonite and kaolinite. Geochimica et Cosmochimica Acta. [Article]. 2013 Sep;117:180-90.

[57] Lutzenkirchen J, Preocanin T, Kallay N. A macroscopic water structure based model for describing charging phenomena at inert hydrophobic surfaces in aqueous electrolyte solutions. Phys Chem Chem Phys. 2008;10(32):4946-55.

[58] Anderson JL. Electrokinetic transport of colloidal particles with heterogeneous surfaces. Journal of Electrostatics. 1995;34(2–3):189-203.

[59] Jiang H, Xie Z, Liu GR, Yu YW, Zhang D. Interaction forces between muscovite and silica surfaces in electrolyte solutions measured with AFM. Transactions of Nonferrous Metals Society of China. 2013 Jun;23(6):1783-8.

[60] Zhao HY, Bhattacharjee S, Chow R, Wallace D, Masliyah JH, Xu ZH. Probing Surface Charge Potentials of Clay Basal Planes and Edges by Direct Force Measurements. Langmuir. [Article]. 2008 Nov;24(22):12899-910.

[61] Liu J, Miller JD, Yin X, Gupta V, Wang X. Influence of ionic strength on the surface charge and interaction of layered silicate particles. Journal of Colloid and Interface Science. 2014 Oct 15;432:270-7.

[62] Lutzenkirchen J. Specific Ion Effects at Two Single-Crystal Planes of Sapphire. Langmuir. 2013 Jun 25;29(25):7726-34.

[63] Cheng L, Fenter P, Nagy KL, Schlegel ML, Sturchio NC. Molecular-Scale Density Oscillations in Water Adjacent to a Mica Surface. Physical review letters. 2001;87(15): 156103.

[64] Kobayashi K, Oyabu N, Kimura K, Ido S, Suzuki K, Imai T, et al. Visualization of hydration layers on muscovite mica in aqueous solution by frequency-modulation atomic force microscopy. The Journal of Chemical Physics. 2013;138(18):184704.

[65] Loh SH, Jarvis SP. Visualization of Ion Distribution at the Mica-Electrolyte Interface. Langmuir. 2010 Jun 15;26(12):9176-8.

[66] Mante P-A, Chen C-C, Wen Y-C, Chen H-Y, Yang S-C, Huang Y-R, et al. Probing Hydrophilic Interface of Solid/Liquid-Water by Nanoultrasonics. Sci Rep. [Article]. 2014;4:6249.

[67] Pashley RM. Dlvo and Hydration Forces between Mica Surfaces in Li+,Na+,K+,and Cs+ Electrolyte-Solutions - a Correlation of Double-Layer and Hydration Forces with Surface Cation-Exchange Properties. Journal of Colloid and Interface Science. 1981;83(2):531-46.

[68] Scales PJ, Grieser F, Healy TW. Electrokinetics of the muscovite mica-aqueous solution interface. Langmuir. 1990 1990/03/01;6(3):582-9.

[69] Lyons JS, Furlong DN, Healy TW. The Electrical Double-Layer Properties of the Mica (Muscovite)-Aqueous Electrolyte Interface. Aust J Chem. 1981;34(6):1177-87.

[70] Yin XH, Yan LJ, Liu J, Xu ZH, Miller JD. Anisotropic Surface Charging of Chlorite Surfaces. Clay Clay Min. 2013 Feb-Apr;61(1-2):152-64.

[71] Nishimura S, Tateyama H, Tsunematsu K, Jinnai K. Zeta-Potential Measurement of Muscovite Mica Basal-Plane Aqueous-Solution Interface By Means of Plane Interface Technique. Journal of Colloid and Interface Science. [Article]. 1992 Sep;152(2):359-67.

[72] Israelachvili JN, Adams GE. Direct Measurement of Long-Range Forces between 2 Mica Surfaces in Aqueous Kno3 Solutions. Nature. 1976;262(5571):773-6.

[73] Pashley RM, Israelachvili JN. Dlvo and Hydration Forces between Mica Surfaces in Mg-2+, Ca-2+, Sr-2+, and Ba-2+ Chloride Solutions. Journal of Colloid and Interface Science. 1984;97(2):446-55.

[74] Pashley RM, Quirk JP. The Effect of Cation Valency on Dlvo and Hydration Forces between Macroscopic Sheets of Muscovite Mica in Relation to Clay Swelling. Colloid Surface. 1984;9(1):1-17.

[75] Yan LJ, Masliyah JH, Xu ZH. Understanding suspension rheology of anisotropically-charged platy minerals from direct interaction force measurement using AFM. Current Opinion in Colloid & Interface Science. 2013 Apr;18(2):149-56.

[76] Yan L, Masliyah JH, Xu Z. Interaction of divalent cations with basal planes and edge surfaces of phyllosilicate minerals: Muscovite and talc. Journal of Colloid and Interface Science. 2013 Aug 15;404:183-91.

[77] Balmer TE, Christenson HK, Spencer ND, Heuberger M. The effect of surface ions on water adsorption to mica. Langmuir. 2008 Feb 19;24(4):1566-9.

[78] Perkin S, Chai L, Kampf N, Raviv U, Briscoe W, Dunlop I, et al. Forces between mica surfaces, prepared in different ways, across aqueous and nonaqueous liquids confined to molecularly thin films. Langmuir. 2006 Jul 4;22(14):6142-52.

[79] Israelachvili JN, Alcantar NA, Maeda N, Mates TE, Ruths M. Preparing contamination-free mica substrates for surface characterization, force measurements, and imaging. Langmuir. 2004 Apr 27;20(9):3616-22.

[80] Nalaskowski J, Abdul B, Du H, Miller JD. Anisotropic character of talc surfaces as revealed by streaming potential measurements, atomic force microscopy, molecular dynamics simulations and contact angle measurements. Can Metall Q. [Article; Proceedings Paper]. 2007 Jul;46(3):227-35.

[81] Sjöberg S, Lövgren L. The application of potentiometric techniques to study complexation reactions at the mineral/water interface. Aquatic Sciences. 1993;55(4):324-35.

[82] Zalac S, Kallay N. Application of mass titration to the point of zero charge determination. Journal of Colloid and Interface Science. 1992;149(1):233-40.

[83] Brezinski DP. INFLUENCE OF COLLOIDAL CHARGE ON RESPONSE OF PH AND REFERENCE ELECTRODES - THE SUSPENSION EFFECT. Talanta. [Article]. 1983;30(5):347-54.

[84] Oman S. A step to a uniform definition and interpretation of the suspension effect. Talanta. 2000;51(1):21-31.

[85] Oman SF. On the seventieth anniversary of the "Suspension Effect": A review of its investigations and interpretations. Acta Chim Slov. [Article]. 2000;47(4):519-34.

[86] Oman SF, Camoes MF, Powell KJ, Rajagopalan R, Spitzer P. Guidelines for potentiometric measurements in suspensions. Part A. The suspension effect (IUPAC Technical Report). Pure and Applied Chemistry. [Article]. 2007 Jan;79(1):67-79.

[87] Schnurr A, Marsac R, Rabung T, Lutzenkirchen J, Geckeis H. Sorption of Cm(III) and Eu(III) onto clay minerals under saline conditions: Batch adsorption, laser-fluorescence spectroscopy and modeling. Geochim Cosmochim Ac. 2015 Feb 15;151:192-202.

[88] Reinholdt M, Miehe-Brendle J, Delmotte L, Le Dred R, Tuilier MH. Synthesis and characterization of montmorillonite-type phyllosilicates in a fluoride medium. Clay Min. 2005 Jun;40(2):177-90.

[89] Tombacz E, Szekeres M. Colloidal behavior of aqueous montmorillonite suspensions: the specific role of pH in the presence of indifferent electrolytes. Appl Clay Sci. [Article]. 2004 Oct;27(1-2):75-94.

[90] Seliman AF, Lasheen YF, Youssief MAE, Abo-Aly MM, Shehata FA. Removal of some radionuclides from contaminated solution using natural clay: bentonite. J Radioanal Nucl Ch. 2014 Jun;300(3):969-79.

[91] Okumura M, Nakamura H, Machida M. Mechanism of Strong Affinity of Clay Minerals to Radioactive Cesium: First-Principles Calculation Study for Adsorption of Cesium at Frayed Edge Sites in Muscovite. J Phys Soc Jpn. 2013 Mar;82(3).

[92] Maslova MV, Gerasimova LG, Forsling W. Surface Properties of Cleaved Mica. Colloid Journal. 2004 2004/05/01;66(3):322-8.

[93] Shubin VE, Kekicheff P. Electrical Double-Layer Structure Revisited Via a Surface Force Apparatus - Mica Interfaces in Lithium-Nitrate Solutions. Journal of Colloid and Interface Science. 1993 Jan;155(1):108-23.

[94] Kekicheff P, Marcelja S, Senden TJ, Shubin VE. Charge Reversal Seen in Electrical Double-Layer Interaction of Surfaces Immersed in 2-1 Calcium Electrolyte. J Chem Phys. 1993 Oct 15;99(8):6098-113.

[95] Abdelmonem A, Lutzenkirchen J, Leisner T. Probing ice-nucleation processes on the molecular level using second harmonic generation spectroscopy. Atmos Meas Tech. 2015;8(8):3519-26.

[96] Liu XD, Cheng J, Sprik M, Lu XC, Wang RC. Surface acidity of 2:1-type dioctahedral clay minerals from first principles molecular dynamics simulations. Geochimica et Cosmochimica Acta. [Article]. 2014 Sep;140:410-7.

[97] Liu XD, Cheng J, Sprik M, Lu XC, Wang RC. Interfacial structures and acidity of edge surfaces of ferruginous smectites. Geochimica et Cosmochimica Acta. 2015 Nov; 168:293-301.